The Pennsylvania State University

The Graduate School

Department of Mechanical Engineering

VEHICLE ROLLOVER PREDICTION FROM LOW ORDER DYNAMIC MODELS OR VARYING TERRAIN ENCOUNTERED DURING MEDIAN TRAVERSAL

A Thesis in

Mechanical Engineering

by

Bridget Catherine Hamblin

Submitted in Partial Fulfillment
of the Requirements
for the Degree of

Master of Science

August 2007

Bridget Catherine Hamblin

The thesis of Bridget Catherine Hamblin was reviewed and approved* by the following:

Sean N. Brennan
Associate Professor, Department of Mechanical Engineering
Thesis Advisor

H.J. Sommer III
Professor, Department of Mechanical Engineering
Thesis Reader

Karen A. Thole
Professor, Department of Mechanical Engineering
Head of the Department of Mechanical Engineering

*Signatures are on file in the Graduate School

ABSTRACT

This work presents an investigation of methods to simulate dynamic behavior of vehicles. The investigation begins with derivations of low-order, linear models used to predict vehicle chassis response. Extensive experimental testing was performed to validate these models. Through validation efforts, the model was modified to include roll dynamics, tire lag and camber influences. Comparisons between model predictions and measured data are presented in both time and frequency domain.

In response to the large effects that terrain had on measured roll dynamics, an investigation on roadway terrain-vehicle interaction was performed. Using commercially available vehicle dynamic software, repeated simulations of median incursions were performed to gain insight on geometric factors that influence a vehicle during a roadway departure. Comparisons of varying median width and varying median front and back slope were conducted. While the simulations offered guidance about profiles that induce harmful situations such as rollover accidents or have the possibility to lead to cross median collisions, a full cost versus benefit analysis would be necessary to determine the ‘best’ median profile.

TABLE OF CONTENTS

LIST OF FIGURES

LIST OF TABLES

ACKNOWLEDGEMENTS

First, I want to thank my parents for their never ending support. Although they may not understand a word of this thesis, it is for them. Without their unwavering faith in my abilities and my dreams, I would never have gotten this far. They have both inspired me to be a better person, driven by a passion for life and a duty to the world. They helped me build a foundation for success, but also gave me the wings to fly. I also want to thank my brother and sister for being wonderful role models, and setting the bar so high. Despite being separated by multiple time zones and often oceans, they were always interested in how and what I was doing. Their love and support could be felt all the way around the globe.

I want to thank the Pennsylvania State University, the Pennsylvania Transportation Institute, the National Science Foundation GK-12 program (Award No: DGE-0338240) and the National Cooperative Highway Research Program for providing the funds and resources for my graduate school experience.

I want to thank all of the staff at the Pennsylvania Transportation Institute, especially those at the test track facility for always being willing to help me with anything and everything, from welding to cleaning the wasps nests out of my car, all without ever making me feel like a stupid girl. The drivers for being very patient during dynamic bus testing, the second shift, especially Rick and Ben, for making me smile at the end of the long days and Dave Fishburn for being a grumpy, but very helpful and caring old man.

To my labmates, current and former, especially Ryan, Vishi and Adam, thanks for getting me through this. . . . . I echo Ryan, that our days in Blue Steel will never be forgotten. If I spend the rest of my career in test vehicles, I cannot imagine I could find a better partner than you. Also, thank you for reminding me that college is supposed to be fun! Vishi, thank you for keeping me sane, helping me debug a million problems, tuning down the spices when cooking Indian food, listening to my pointless stories, but most importantly, being my friend. Adam, thank you for always telling me when there were

treats down the hall, for our lunch conversations about nothing, for always listening and for helping me through many tough times. I hope my actions will help you endure.

To my GREATT friends, study buddies, and the other wonderful people I have met in my short time in Happy Valley, thank you for keeping the play hard in balance with the work hard. I wish I could've stayed longer just to be with you all.

Thank you to Dr. Eric Donnell for sharing your wisdom about highway design with me and to Dr. Joe Sommer for being my reader.

To my advisor, Dr. Sean Brennan, I quote Christina Aguilera's *Fighter*, 'if it wasn't for all of your torture I wouldn't know how to be this way now, and never back down, so I wanna say thank you cause it makes me that much stronger…so thanks for making me a fighter.'

Chapter 1

Introduction

Vehicular rollover is a tragedy that is continually gaining public interest. The issue is amplified by the ever increasing numbers of large trucks and Sport Utility Vehicles (SUV's), which carry the highest rollover probability of any type of vehicle, more than twice the rollover probability of smaller passenger vehicles [1]. Despite the public knowledge concerning the rollover potential of large vehicles, they are still increasing in numbers [2]. In an effort to better understand vehicular rollover, this thesis examines means to predict vehicle behavior, including rollover, based on a driver's steering input and the terrain encountered by the vehicle, especially after roadway departure.

1.1 Motivation

Studies concentrating on vehicular safety started shortly after the first automobile was produced. While many safety programs concentrate on the driver's behavior, such as seat-belt and drunken driving campaigns, the driver is the most difficult factor of vehicular safety to control. Therefore, much of the responsibility for vehicular safety falls on automobile manufacturers and traffic engineers. Auto manufacturers usually concentrate on making vehicles safer when involved in accidents, but have recently switched their thinking to focus more on preventative safety measures.

This recent change in approach to transportation safety is fueled by an increase in rollover accidents over the last decade. Between 1996 and 2005, rollover accidents increased in occurrence, from 2.3% of all accidents to 2.6% of all accidents [1, 3]. Passenger cars rolled over in approximately 2% of all accidents in 2005 while utility vehicles rolled over in approximately 5% of all accidents [1]. This was even a decrease compared to a rollover rate for utility vehicles in all accidents of 6% in 2000 [4]. But

even with the high rate of rollovers, SUV's continue to increase in numbers. The National Household Travel Survey didn't even have a category for SUV's until 1995, when SUV's made up fewer than 7% of the vehicles on the roadway. The latest survey, conducted in 2001, found that SUV's now account for over 12% of all vehicles [2]. So it is not surprising that the number of rollover accidents over the last decade has increased. This slight increase in rollover occurrences is also accompanied by an increase in fatalities resulting from rollovers. In 1996, 18.3% of the fatal accidents were the result of a vehicle rollover while in 2005, 21.1% of the fatal accidents were due to rollover [1, 4]. This correlates to an additional 1,434 lives lost each year from the increase in rollover accidents [1].

Utility vehicles growing popularity even despite the high likelihood of being involved in a rollover accident is shifting the source of fatal accidents on the nation's roadways. Light trucks, which include pickup trucks, utility vehicles and vans, accounted for 31.8% of the fatalities in 1996 but 38.5% of the fatalities in 2005 while fatalities in passenger cars decreased from 53.5% to 42.2% over the same period [1, 3].

There are many other factors that can affect a vehicle's likelihood to rollover besides its own geometric configuration. Accident location can play a large role in the onset of a rollover event. Even though the number of accidents is on the decline, the number of accidents occurring off the roadway has not decreased at the same rate [5]. Off road accidents prove to be more dangerous than those that take place on the roadway with the introduction of roadside obstacles and varying terrain. While only 24.5% of all accidents in 2005 took place off the roadway, 75% of all fatal accidents took place off the road [1]. A large factor in off-road accidents is the increased rollover probability. The National Highway Traffic Safety Administration estimates that 90% of rollover accidents are tripped events, often induced by the vehicle leaving the roadway [6]. Therefore, most of the effort in highway redesign is being concentrated on the roadside profile. The idea of the forgiving roadside was first presented decades ago, but standards for a forgivable roadside have not been updated to account for the recent dramatic shift in the types of vehicles on the roadway.

1.2 Idea of Prevention by Vehicle Control

As Ben Franklin said, ‘An ounce of prevention is worth a pound of cure.’ While this idea has been carried over into almost every facet of life, it carries more weight when dealing with preventing causes of serious injury or death, such as vehicular accidents. While automobile manufacturers are continually trying to make vehicles safer when involved in an accident by installing air bags in the front and rear, three-point seat belts for every seat and reinforcing the sidewalls to withstand greater amounts of force, they are also starting to focus on accident prevention. One of the first attempts to aid the driver in avoiding accidents was the installment of Anti-lock Brake Systems (ABS). A more recent step in preventing automobile accidents has been the implementation of Electronic Stability Control (ESC), which controls braking to maintain yaw stability of the vehicle. Both ABS and ESC use an onboard computer to monitor wheel slip and in the case of ESC, also vehicle yaw angle, and then distributes brake pressure to stabilize the vehicle while maintaining driver control. As computing capabilities continue to increase, researchers are looking for additional means to further increase vehicular safety.

One area of interest is in predicting the roll angle of a vehicle with the idea that if a computer can first predict rollover, it can direct measures to prevent rollover. To predict roll behavior of a vehicle, researchers have developed governing equations of motion for vehicles based on two easily measured driver inputs, steering angle and velocity. Such equations should remain low-order and linear in order to be easily implemented for control purposes. Because of this, researchers often start their investigation with a two degree of freedom (2-DOF) representation of vehicle motion, often called the bicycle model [7]. From this simple representation, corrections to include roll dynamics are often added with a goal of minimizing model complexity. While many researchers have derived such numerical models of vehicular behavior, few have validated their models.

The first part of this work involved deriving similar governing equations of motion to those presented by other researchers and then validating the models using experimental data. Through the validation process, the models were improved to better capture a vehicle’s dynamic response in a variety of maneuvers. A large part of this work

is based on the foundation of two previous students, John Cameron and Ryan Martini [8, 9]. John performed some preliminary studies of roll dynamics and Ryan created a highly accurate data acquisition system useful in vehicle dynamic studies. This work differs significantly from this previous work in the depth of investigation regarding roll dynamics. The use of the new data acquisition system allows for increased confidence in the data and as this thesis will illustrate, sheds light on additional influences on vehicular behavior.

1.3 Idea of Prevention by Roadway Design

Possible redesign of the nation's roadways is another avenue that researchers are investigating as a means to prevent fatal accidents. Such work is recently motivated by the large increase of rollover accidents occurring within highway medians. This reactive mentality is commonplace in highway design due to the significant cost associated with design changes. Any alterations in design or barrier placement must often be evaluated over a period of years or decades to determine if it will make a statistical difference in the severity of accidents.

With today's expanding knowledge about modeling vehicle dynamics, it seems beneficial to look at a vehicles response during a median incursion prior to implementation of design changes. Thus, simulations can reveal shortcomings in the design before anyone is injured or killed due to the implementation. Through repeated experimentation and data analysis, one can analyze the influence of varying terrain on the dynamics of a vehicle.

This work explores the use of simulations to analyze how drastic terrain variations such as roadway shoulders and medians, which would be very expensive and dangerous to physically test, affect vehicle safety. To continue this investigation, a more complex vehicle dynamics simulation package was used that better accounts for terrain variability, something that was ignored in the previously mentioned bicycle model. The commercially available CarSim® software [10] was used to model median incursions from divided highways for multiple configurations in efforts to gain insight about better

median profiles for the updated fleet of vehicles on the roadway today. This analysis has suggested relationships between median designs and vehicle safety and suggests improvements that do a better job at entrapping vehicles without inducing a rollover event. A significant contribution of this thesis is that such extensive analysis has not been published in the literature prior to this work.

1.4 Outline of Remaining Chapters

This thesis is motivated by a desire to decrease the number of rollover accidents by predicting rollover based on driver inputs and terrain features. The background, methodology and results are presented in the following chapters, with the breakdown explained below.

Chapter 2 presents a literature review of past work in the area of low-order, linear models of dynamic rollover behavior and the past use of vehicle dynamic simulations. Methods of predicting vehicle behavior during a median incursion commonly used in the field of highway engineers is also presented.

Chapter 3 presents derivations of the 2-DOF bicycle model and three degree of freedom (3-DOF) roll dynamics models. The testing and validation process are outlined and the results presented in Chapter 4. Modifications to the derived models are supported in detail with experimental data.

Chapter 5 presents the methodology and results of a study on the effects of median width and slope on a vehicles response during a roadway departure. Chapter 6 offers reflections on the work presented in this thesis along with recommendations for future work in the area.

1. *Traffic Safety Facts 2005: A Compilation of Motor Vehicles Crash Data from the Fatality Analysis Reporting System and the General Estimates System*. 2006, U.S. Department of Transportation: National Highway Traffic Safety Administration: Washington, D.C.
2. *2001 National Household Travel Survey: Summary of Travel Trends*. 2004, U.S. Department of Transportation.
3. *Traffic Safety Facts 1996: A Compilation of Motor Vehicle Crash Data from the Fatality Analysis reporting System and the General Estimates System*. 1996, U.S. Department of Transportation: National Highway Traffic Safety Administration: Washington, D.C.
4. *Traffic Safety Facts 2000: A Compilation of Motor Vehicle Crash Data from the Fatality Analysis Reporting System and the General Estimates System*. 2001, U.S. Department of Transportation: National Highway Traffic Safety Administration: Washington, D.C.
5. McGinnis, R.G., Davis, Matthew J., Hathaway, Eric A., *Longitudinal Analysis of Fatal Run-Off-Road Crashes, 1975 to 1997*. Transportation Research Record, 2001. **1746**: p. 47-58.
6. NHTSA, *Vehicle Dynamic Rollover Propensity Project Overview: http://www-nrd.nhtsa.dot.gov/vrtc/ca/rollover.htm*. 2004.
7. Bundorf, R.T., *A Primer on Vehicle Directional Control*. 1968, Warren: General Motors Technical Center: Michigan Engineering Publication.
8. Cameron, J.T., *Vehicle Dynamic Modeling for the Prediction and Prevention of Vehicle Rollover*, in *Mechanical Engineering*. 2005, Pennsylvania State University: University Park.
9. Martini, R.D., *GPS/INS Sensing Coordination for Vehicle State Identification and Road Grade Positioning*, in *Department of Mechanical and Nuclear Engineering*. 2006, Pennsylvania State University: University Park.
10. CarSim, *Mechanical Simulation Corporation*. 2006. http://www.carsim.com.

Chapter 2

Literature Review of Vehicle Dynamic Simulations

Modeling of vehicle behavior has been an area of interest since the invention of the automobile. Modeling allows a designer to examine the results of their invention, and allows automobile designers to investigate the dynamic behavior and safety of their products. While efforts to model the dynamic behavior of automobiles have progressed over the past decade, the accuracy and capabilities of simulations have increased exponentially with breakthroughs in computer technology. Computer simulation tools allow the designer to investigate a vehicle's safety and performance without ever having to build or test the vehicle, both of which are very costly endeavors. Vehicle dynamic simulation software has been a crucial part in vehicle design and safety for many decades in three primary application areas:

1. Automotive designers who utilize software to predict possible problems with new designs and existing systems,
2. Government agencies who rely on simulation software to aid in determining if a new vehicle is safe and to analyze testing protocols, and
3. Forensic engineers who use the simulations to pinpoint chain of events in accidents.

This work justifies the use of simulations by first investigating and validating low-order linear models of vehicular behavior. Fueled by observations during the validation process, this work then pushes the capabilities of simulations to yet another facet of application of vehicle dynamic simulation:

4. Highway design engineers who could use simulations to predict relationships between roadway geometry, median geometry in particular, and resulting crash types and incident rates.

Because this last use of vehicle dynamic simulations is a relatively new approach, an overview of the literature and state-of-the-art is described in detail in this chapter. Particular attention is given to describe challenges or obstacles that might occur when software developed for the first three application areas is used in the fourth.

The quantity of material describing vehicle dynamic behavior is much too extensive to allow a comprehensive presentation in one chapter, or even one publication. This literature review therefore focuses on dynamic simulations of vehicle behavior that relate to justifications of this new approach to simulations. The chapter first presents a history of vehicle dynamic simulations including the three pathways of development. A historical background on cost versus benefit software programs employed by highway designers is also presented. This is followed by a description of common simulation packages in use today. Methods used to validate the software are then described, leading to a discussion of issues associated with use of dynamic simulation software for highway geometry design. These issues are grouped into three general categories: 1) validation, 2) accident reconstruction, and 3) tire-soil interaction.

2.1 Historical Use of Vehicle Dynamic Simulations

To recognize the complexity of simulations, one only needs to consider how simulations function. Vehicle simulations use numerical solvers to calculate outputs from a set of inputs using both differential equations derived from laws of physics and physical and geometrical constraints of the vehicle. An overview of simulation technology can be found in [1-5].

The dominant usage of vehicle simulations today remains the study of vehicle handling and response. While numerical dynamic models of vehicle behavior have been presented in literature as far back as the 1950's, their usage was generally limited by the inability to solve the often complex equations of motion on limited computing hardware [6, 7]. Since the development of low-cost personal computing in the past several decades, simulations have become commonplace in the study of vehicle motion.

For this particular study of vehicle rollover and terrain induced rollover, there are fortunately a limited number of primary factors which dominate vehicle behavior. By “primary factors”, it is meant that these factors dominate the overall chassis motion of the vehicle. In addition to variable terrain geometry, these primary factors might include chassis inertial parameters, gross tire-soil interaction effects, and overall suspension stiffness.

In many cases, there is a non-trivial amount of uncertainty in the primary factors that govern vehicle motion, so that inclusion of secondary or tertiary predictors of vehicle behavior such as the dynamics of the power steering unit, is not productive. For example, assume that 97% of bulk motion of the vehicle is predicted by a small set of core equations and parameters. If the parameters entering this equation have an uncertainty such that the predicted output varies by 10%-20%, then inclusion of additional factors to gain additional 3% of fidelity for one particular vehicle might not be fruitful.

LeBlanc et al during their research regarding lane detection illustrated the effects of adding complexity to simulation models [8]. Shown in Figure **2.1** is a comparison of a 2-DOF linear tire model and a 14-DOF Magic Tire model.

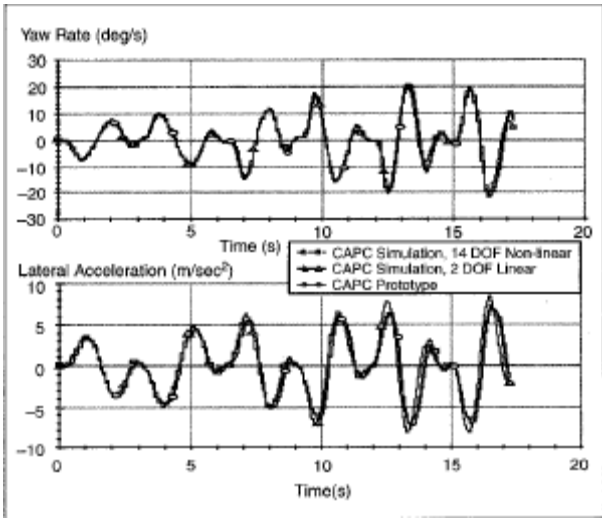

Fig. **2.1**: Comparison of Tire Models

While some additional accuracy is gained at higher magnitudes of lateral acceleration, the simple 2-DOF model does an adequate job of simulating the vehicle's response.

As computational capabilities have increased, so has the development of more complex and realistic vehicle simulations [9-11]. For example, in [9], Day recounts the state-of-the-art in simulation programs of the late 1980's, summarizing respective strengths and weaknesses of various simulation programs at that time. The choices were clearly partitioned between either vehicle dynamics applications or crash-reconstruction applications in the form of impact simulations. By the 1990's, the convergence of impact-analysis type software and vehicle dynamics was facilitated by the availability of finite element modeling, better inclusion and understanding of tire and impact forces, better analysis of tripping/furrowing effects, and better validation of tire models for large variations in camber and normal force. Simulations emerged that were able to model rollover behavior from the initial trajectory as the vehicle leaves a roadway, through an off-road segment into a rollover situation. Today, road profile and similar 3D effects have been incorporated into most commercial simulation environments with claims of close fidelity between simulation-predicted vehicle behavior and experimental measurements[9, 12].

The concept of applying vehicle dynamics software to the analysis of off-road vehicle behavior is gaining recent popularity. For example, some researchers have used simulations to study driver response to roadway departure [13]. Others have concentrated on off-road ride comfort [14] and some have focused on friction influences due to water or snow [15]. While these applications are diverse, few people to date have looked specifically at the use of vehicle dynamics to analyze and optimize the roadway design itself. This thesis is one of the first to present an extensive study of vehicle dynamics on off-road behavior across a wide range of vehicles and terrain features.

2.2 Historical Use of Cost/Benefit Highway Design Tools

Highway engineers have been using simulation programs for decades as a means to calculate the cost versus benefit value for changes in roadway designs. Such programs

usually use accident data to estimate encroachment frequency, accident frequency, severity and the resulting cost of the accident, including both injury cost and the cost to repair any damaged obstructions. Such cost/benefit programs have progressed over the years to include updated encroachment data, accident data and to improve the program's user interface in hopes of increasing the programs usage. The Texas Transportation Institute released the ABC program in the mid-1980's; a cutting edge program at the time for it used the then recent results of the Cooper encroachment study [16]. The ABC program was also capable of predicting results for four vehicles and incorporated a two-step approach in predicting injury severity by first calculating impact severity under suspected conditions for a given barrier. The Federal Highway Administration modified TTI's ABC program to make it more user friendly and improve the crash severity models and released the update in 1988 as the Benefit/Cost Analysis Program (BCAP). BCAP is most well known because it was used to develop the guidelines outlined in the 1989 AASHTO Guide Specifications for Bridge Railings. The BCAP program used inputs derived more from engineering judgment than from concrete data. While it predicts encroachment and speed distributions that differ from measured data, it has means to better account for impacts with roadside hardware.

Continual refinement and a push for fewer required user defined inputs led to the development of ROADSIDE, published as an appendix in the 1996 Roadside Design Guide [17]. But the program proved to be oversimplified to adequately model roadside incursions. The National Cooperative Highway Research Program recognized ROADSIDE's shortfalls, so funded a project to develop a replacement program. The Roadside Safety Analysis Program (RSAP) was produced by the Texas Transportation Institute and included in the updated 2002 Roadside Design Guide [18]. While case studies of the RSAP program show some correlation between model predictions and accident data, the program relies mostly on accident history as inputs, making it difficult to update the program to account for changes in the vehicle fleet and it completely ignores driver input and the resulting dynamic response [19].

Other researchers have developed their own cost versus benefit tools independent of those mentioned above. In the mid-1990's, a research group from the University of

British Columbia completed an overhaul of the Roadside Hazard Simulation Model, a program originally developed in the 1970's using Cooper's encroachment data [20]. The updated version allowed for limited driver inputs such as corrective steering and braking to be considered when determining the likely outcome of the roadway departure. Ray also developed a cost versus benefit tool in the mid-1990's called Safety Advisor [21]. It had the unique feature of allowing the user to input probability distributions of encroachments and accident severity. This allowed the user to tailor the program to the specific roadway under review.

2.3 Common Vehicle Dynamics Simulation Packages

The development of vehicle dynamic simulations over the past several decades has progressed along many parallel lines and applications, but the goal in using simulations is always to alleviate the cost, time, safety, and availability concerns associated with experimental testing. One line of development is in the area of vehicle design where simulations are used to aid in vehicle setup, stability analysis, and performance. Modern examples of software focusing on this area of implementation include CarSim, TruckSim, HVOSM and VDANL [22-25]. Many of these programs have been extended in the past several years, allowing them to perform other tasks, for example accident reconstruction. Another line of development of vehicle simulation software programs were programs originally developed with the specific goal of aiding in accident reconstruction, for example PC-Crash and HVE [26, 27]. Many of these accident-reconstruction software packages today are fully capable of simulating extensive off-road and on-road driving scenarios even apart from the crash event itself. A third area of development has utilized finite element analysis. The most common vehicle FEA package is LS-DYNA which has been used extensively in the field of barrier testing [28, 29]. Thus, these converging capabilities across vehicle dynamics analysis and crash reconstruction applications present a new and powerful toolset to the roadway designer. An overview of popular software packages available follows:

- VDANL – Systems Technology Inc. [25]
    - **V**ehicle **D**ynamics **A**nalysis, **N**on **L**inear
    - Originally developed for vehicle dynamics simulation
    - Has been expanded to some accident reconstruction applications
- ADAMS – MSC Software [22]
    - Originally developed for multi-body simulations, but adapted recently for vehicle applications
    - Entire car and environment has to be built piece by piece
    - Has recently updated tire models to allow for better 3-D road profiles
- CarSim – Mechanical Simulation Corporation [23]
    - Originally developed for vehicle design/dynamic simulation purposes
    - Can input 3-D terrain profiles and friction coefficients
    - Can select from several tire models, or create your own
- HVOSM –McHenry Software [24]
    - **H**ighway **V**ehicle **O**bject **S**imulation **M**odel
    - Originally developed for vehicle simulation in the mid-60's
    - Several updates and validations have been done since then
    - McHenry adapted and targeted more towards accident reconstruction
- PC-Crash – MEA Forensic Engineers and Scientists [26]
    - Collision software that also handles rollover
- HVE – Engineering Dynamics Corporation [27]
    - Has several modeling options available
    - Both single vehicle dynamics and multiple vehicle collisions
    - Has a new Soft-Soil tire model that can be applied to individual wheels to deal with sinkage and plowing
- LS-DYNA – ANSYS [30]
    - FEA software to model impacts and deformation
    - Commonly used in highway barrier design and testing

Each of the software packages has relative strengths and weaknesses which stem from the historical development of the software and expected use of the simulation results.

2.4 Validation of Vehicle Dynamics Simulation Software

The main purpose in using a vehicle dynamics simulation is to replace extensive experimental testing with simulation. This alleviates cost, time, and road/vehicle availability concerns. But in order to replace experimental data, the simulation must be able to accurately predict the outcome of experimental tests. Historically, there are long-standing discussions and exchanges in literature that either question or assert the fidelity of vehicle dynamic simulations to real-world behavior. The confirmation that a simulation is correctly describing the behavior of the system for which it is intended is hereafter called "validation." A claim that a simulation's prediction is valid, of course, depends strongly on the application area and the desired level of accuracy of the model prediction.

The necessity of validation isn't always clearly stated in a simulation study or software package. Some have argued that the use of a simulation as a tool always requires a corresponding validation process [10]. Others point out that the scarcity of experimental data makes this a difficult requirement [31]. Some users of refined simulation software packages claim validity by illustrating similarities to older simulation models without comparison to actual data [32]. Almost all the software currently available has been validated to some extent, but few have met the rigorous standards that have been proposed, for example, by Heydinger [32].

Additionally, some researchers have noted that validation depends on the process used to obtain the model fit itself. This brings into question whether the same data used to obtain vehicle parameter fits should be used to claim validity of the model. Heydinger, in [32], presents a methodology for validation of vehicle dynamics simulations and points out many faults of recently presented validations.

Possible bias due to the vested interest of the evaluator and the choice of vehicle for real-world comparisons are sometimes discussed as factors influencing the validation process. Ideally, validation should be achieved through repeated testing of several vehicles performing a variety of maneuvers, a method proposed by Heydinger. However, this requirement is so difficult that there are few if any vehicle simulation codes that would satisfy this condition. There is at least recognition of possible bias in validation and consequently some validations have been performed by third parties [32]. However, the majority of simulation/data comparison has been published by the software creator [10] [33].

One fact illustrating the difficulty in validation is the limited availability of instrumented crash data. Many software packages claim validation using the same data set that came from Failure Analysis Associates Inc. Test and Engineering Center. Eight different rollover tests were performed and presented in [34]. Five of the tests were curb tripped rollovers, two were soil tripped and one was a dolly test. Roll angle, vertical, horizontal and angular velocities along with total energy were determined for each test using instrumentation within the car and post-processing with high-speed photography. The results from such testing were once considered valid representations of rollover situations, but the severity levels have come under question, causing most companies to seek out other test results or perform their own small set of experiments to help validate their models [34-37]. Other programs designed for reconstruction purposes perform some of their validation through reconstructions of documented accidents .

Several papers exist in the literature validating the aforementioned simulation codes along the progression of their capabilities. A short list is supplied for each of the software programs discussed in this review.

- VDANL – Systems Technology Inc. [33] [38, 39]
- ADAMS – MSC Software [40-42]
- CarSim – Mechanical Simulation Corporation [5, 39]
- HVOSM –McHenry Software [27] [43]
- PC-Crash – MEA Forensic Engineers and Scientists [44-47]
- HVE – Engineering Dynamics Corporation [9-11, 27]

- LS-DYNA – ANSYS Inc. [28, 29]

There are many commonalities among the validations besides often relying on the same rollover data [34]. The same maneuvers are often used including J-turns, sinusoidal steer, double lane changes and braking in a turn [11, 32]. These maneuvers primarily focus on aggressive handling and nonlinear dynamics, and hence the comparisons are historically all presented in the time domain. A drawback to this approach is the limited attention given to the behavior of the vehicle in the transition to nonlinear behavior and during high frequency transients. For example, frequency responses are rarely if ever considered or checked for linearity even though many validation approaches include a sinusoidal steering input. The drawback of only examining the time domain matches will be explained further in the next section.

2.5 Challenges to Using Vehicle Dynamic Simulations to Predict Vehicle Behavior in Medians

2.5.1 Shortfalls in Validation

Sometimes the simulation will appear to match one set of data yet mismatch another, making the method used for validating a model important. There are two common methods for comparing experimental and predicted results of a system: time domain and frequency-domain. Time domain analysis examines the output as a function of time and is useful to illustrate general trends or nonlinearities, while the frequency domain analysis can be used to confirm the linearity of a system's response by plotting the ratio of the outputs magnitude and phase compared to the input against the frequency of the input signal. This is useful to illustrate types or frequencies of inputs where model matching will and will not be obtained.

As mentioned previously, most of the validation work regarding simulation software has been done in the time domain. Slight discrepancies between simulated and actual data may not seem severe in the time domain, but the differences become more

defined when taken to the frequency domain, especially at higher frequencies where excitation of higher-order dynamics, especially roll is more pronounced. As an example of this, Figure **2.2** below shows the yaw rate response of a 1987 Hyundai Excel in the time domain [32]. The plot shows a good correlation between the measured data and the simulation.

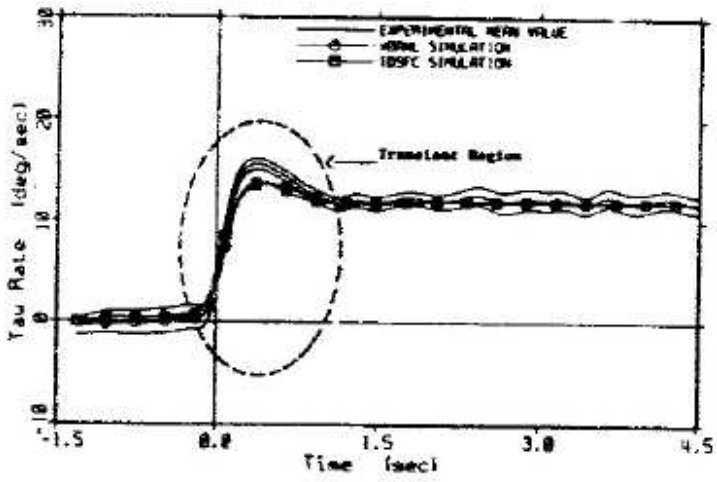

Fig. **2.2**: Yaw rate response in time domain

Figure 2.3 is the yaw rate frequency response of the same car. While the time domain fits appear to be in agreement, the frequency domain plots illustrate more clearly the discrepancies between the measured data and the simulation by including a wider range of inputs.

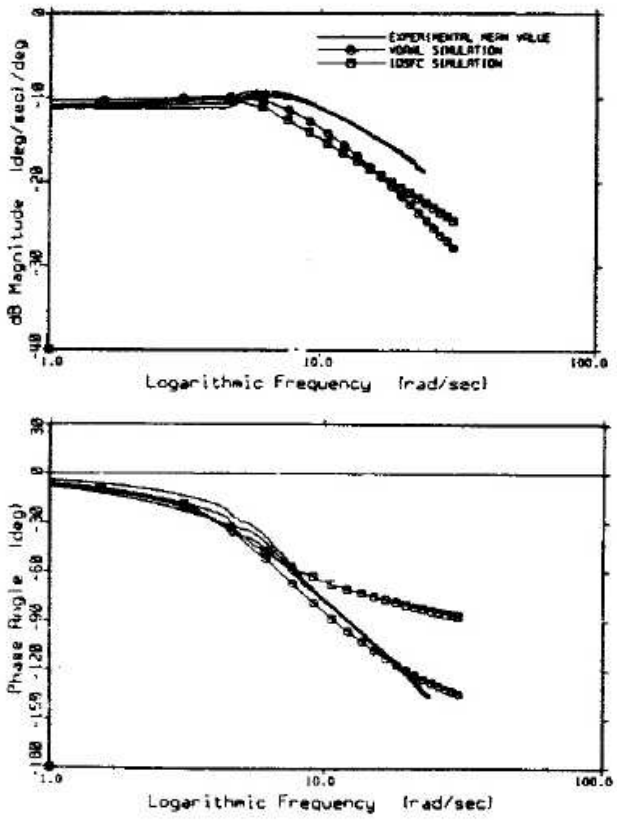

Fig. 2.3: Yaw rate response in frequency domain

Another factor that can lead to questioning of the validity of a model comparison is the expected errors that arise out of experimental data collection. Even under controlled situations, natural disturbances such as wind gusts or road roughness can affect the measured values of a vehicle. Heydinger recommends running numerous tests for a given data point, selecting those that best match the targeted maneuver and averaging the values of the measurements [32]. The use of averaged values of inputs such as steering torque is intended to reduce the effects of the natural disturbances that will not show up in any simulation. To increase the validity of the comparison, it is important that the

simulation and data match for not only different types and severities of maneuvers but also for different vehicles [32].

Correlations between measured and predicted values are often difficult to quantify, so Heydinger suggests using many simultaneous measures of validation [32]. Including 95% confidence intervals on each side of the measured data can provide a visual tool to aid in determining validity in the presence of measurement uncertainty. Another range of acceptable simulated results could be created by averaging the error due to natural disturbances and using that error value as a limit for validation.

Perhaps the largest area of concern regarding validation is the data used for the validation. The public outcry for updated crash test data has grown louder in recent years especially in the area of rollover, where a standardized test has yet to be selected [3] [45]. The dolly test outlined in FMVSS 208 was previously used as a standard rollover test [35]. In this test, the car would be accelerated sideways while sitting on a dolly inclined at 23° until the car reaches 30 mph at which point the dolly hits a stop and the car flips off and rolls over. While the dolly test ensures that rollover occurs, the lack of repeatability of such testing has raised questions about its validity. Parenteau et al studied trends in rollover accidents and concluded that soil-trip rollovers account for 51.7% of all passenger car rollovers, but the dolly test induces roll rates much higher than actual field conditions and is unable to adequately model soil-tripped or curb-tripped rollovers [35].

2.5.2 Shortfalls in Simulations Regarding Accident Reconstruction

One shortfall that is often overlooked is the reliance on simulations to clarify previous events. Some authors, Day for instance [9], stress the importance of remembering that when a simulation correlates with the evidence of events left on the roadway (for a crash reconstruction analysis), it does not rule out all other possibilities of behavior. It simply presents one possibility. It is sometimes possible for different combinations of inputs to produce equivalent simulation outputs that fall within the bounds of validation for a given event.

Day also points out that inputs to the system during an accident are unknown values that must be determined from the outcome of the event. Problems arise particularly in vehicle reconstruction work because many software programs do not allow for steering inputs during and after a collision. This is true even though in some instances a driver still has some control over the trajectory of their vehicle. This unknown steering input could greatly affect the actual trajectory or estimated speeds of the vehicles, as will be shown in great detail later in this thesis.

2.5.3 Shortfalls Due to Inadequate Tire Models

One of the most challenging aspects in predicting vehicle dynamic behavior is the creation and validation of tire models describing off-road behavior [38]. The general field of terrain-vehicle interaction is called terramechanics, and is a well developed area of research dating back to the 1940's and '50's. In 1969, Mieczyslaw Bekker published what is today considered one of the preeminent publications on the subject [48]. Even though his studies on the influences of off-road terrain has been acknowledged for quite some time, Bekker's findings have only recently been implemented in vehicle simulations and validated for use in highway situations. This inclusion can greatly increase the accuracy of simulations modeling off-road vehicle trajectories. While an accurate tire model is mandatory for accurately simulating off-road dynamics, Metz points out that in off-road situations, terrain has a much larger effect on tire forces than the properties of the tire themselves [49]. Other large off-road influences include an increase in tire lag due to softer terrain and tire sinkage affecting both sidewall and longitudinal forces. The plowing effects of the tire adds complexity to the tire model which not all programs, including PC-Crash have been able to correctly model [45]. Most simulation programs have recently updated their tire models to better incorporate off-road effects but many of these improvements have not yet been validated publicly [38, 44]. Such improvements are critical for rollover studies since 90% of rollover accidents occur off-road or in transitions from on-road to off-road driving. This therefore

challenges the development of simulations of off-road driving as a tool in preventing rollover accidents [31].

2.6 Conclusions

This chapter presented a history of vehicle dynamic simulation packages and a history of cost/benefit highway design tools to provide the groundwork for the ideas to be discussed in the following chapters. Starting with simple linear equations of motion, dynamic modeling has progressed together with computing capabilities. The automotive sector, highway design community and the general public have all benefited from the advances in modeling capabilities. While much progress has been made, limitations still exist especially in modeling uncommon situations such as off-road terrain and rollover events.

1. Sayers, M.W., Mousseau, C.W., *Real-Time Vehicle Dynamic Simulation Obtained with a Symbolic Multibody Program.* ASME - Applied Mechanics Division, 1990. **108**: p. 51-58.
2. Kortum, W., Sharp, R.S., ed. *Multibody Computer Codes in Vehicle System Dynamics: Supplement to Vehicle System Dynamics, Vol 22*. 1993, Swets & Zeitlinger B.V.: Amsterdam.
3. Chou, C.C., Wu, F., Gu, L., Wu, S.R., *A Review of Mathematical Models for Rollover Simulations.* ASME - Applied Mechanics Division, 1998. **230**: p. 223-239.
4. Wei-qun, R., Yun-qing, Z., Guo-dong, J., *A New Application of Multi-Body System Dynamics in Vehicle-Road Interaction Simulation.* Wuhan University Journal of Natural Sciences, 2003. **8**(2A): p. 379-382.
5. Sayers, M.W., Han, D., *A Generic Multibody Vehicle Model for Simulating Handling and Braking.* Vehicle System Dynamics Supplement, 1996. **25**: p. 599-613.
6. Segel, L., *Research in the Fundamentals of Automobile Control and Stability.* SAE 570044, 1957.
7. Bundorf, R.T., *A Primer on Vehicle Directional Control*. 1968, Warren: General Motors Technical Center: Michigan Engineering Publication.
8. LeBlanc, D.J., Johnson, G.E., Venhovens, P.J., Gerber, G., DeSonia, R., Ervin, R., Lin, C-F., Ulsoy, A.G., Pilutti, T.E., *CAPC: A Road-Departure Prevention System*, in *IEEE Control Systems Magazine*. 1996, p. 61-71.
9. Day, T.D., Hargens, R.L., *Application and Misapplication of Computer Programs for Accident Reconstruction.* SAE 890738, 1989.
10. Day, T.D., Siddall, D.E., *Validation of Several Reconstruction and Simulation Models in the HVE Scientific Visualization Environment.* SAE 960891, 1996.
11. Day, T.D., *Validation of the EDVSM 3-Dimensional Vehicle Simulator.* SAE 970958, 1997.
12. DeLays, N.J., Brinkman, C.P., *Rollover Potential of Vehicles on Embankments, Sideslopes, and Other Roadside Features.* SAE 870234, 1987.
13. McMillan, N.J., Pape, D.B., Hadden, J.A., Narendran, V.K., Everson, J.H. *Statistics-Based Simulation Methodology for Evaluating Collision Countermeasure Systems Performance*. in *IEEE Conference on Intelligent Trasportation Systems*. 1998.
14. Claar, P.W., Buchele, W.F., Sheth, P.N., *Off-Road Vehicle Ride: Review of Concepts and Design Evaluation with Computer Simulation.* SAE 801023, 1980.
15. Mancosu, F., *Vehicle-Road-Tyre Interaction in Potential Dangerous Situations: Results of VERT Project.* SAE 2002-01-1181, 2002.
16. Mak, K.K., Sicking, Dean L., *NCHRP 492 - Roadside Safety Analysis Program (RSAP) - Engineer's Manual*. 2003, Transportation Research Board: Washington, D.C.
17. *Roadside Design Guide*. 1996, American Association of State Highway and Transportation Officials: Washington, D.C.
18. *Roadside Design Guide*. 2002, American Association of State Highway and Transportation Officials: Washington, D.C.

19. Khasnabis, S., Naseer, Mubashir, Baig, Mirza F., Opiela, Kenneth S., *Roadside Safety Analysis Program as a Tool for Economic Evaluation of Roadside Safety Projects.* Transportation Research Record, 1999. **1690**: p. 31-41.
20. deLeur, P., Abdelwahab, W., Navin, F., *Evaluating Roadside Hazards Using Computer-Simulation Model.* Journal of Transportation Engineering, 1994. **120**(2): p. 229-245.
21. Ray, M.H., *Safety Advisor: Framework for Performing Roadside Safety Assessments.* Transportation Research Record, 1994. **1468**: p. 34-40.
22. ADAMS, *MSC Software*. 2006. http://www.mscsoftware.com.
23. CarSim, *Mechanical Simulation Corporation*. 2006. http://www.carsim.com.
24. HVOSM, *McHenry Software*. 2006. http://www.mchenrysoftware.com.
25. VDANL, *Systems Technology Inc.* 2006. http://www.systemstech.com.
26. PC-Crash, *MEA Forensic Engineers and Scientists*. 2006. http://www.maceng.com.
27. HVE, *Engineering Dynamics Corporation*. 2006. http://www.edccorp.com.
28. Consolazio, G.R., Chung, Jae H., Gurley, Kurtis R., *Impact Simulation and Full Scale Crash Testing of a Low Profile Concrete Work Zone Barrier.* Computers and Structures, 2003. **81**: p. 1359-1374.
29. Omar, T.A., Kan, Cing Dao, Bedewi, Nabih E., Eskandarian, Azim, *Major Parameters Affecting Nonlinear Finite Element Simulations of Vehicle Crashes.* ASME - Applied Mechanics Division, 1999. **237**: p. 1-17.
30. LS-DYNA, *ANSYS Inc*. 2007. http://www.ansys.com/products/lsdyna.asp.
31. Viano, D.C., Parenteau, C., *Case Study of Vehicle Maneuvers Leading to Rollovers: Need for Vehicle Test Simulating Off-Road Excursions, Recovery and Handling.* SAE 2003-01-0169, 2003.
32. Heydinger, G.J., Garrott, W.R., Chrstos, J.P., Guenther, D.A., *A Methodology for Validating Vehicle Dynamics Simulations.* SAE 900128, 1990.
33. Allen, R.W., Chrstos, J.P., Howe, G., Klyde, D.H., Rosenthal, T.J., *Validation of a Non-Linear Vehicle Dynamics Simulation for Limit Handling.* IMechE 2002 Special Issue Paper, 2002.
34. Cooperrider, N.K., Thomas, T.M., Hammoud, S.A., *Testing and Analysis of Vehicle Rollover Behavior.* SAE 900366, 1990.
35. Parenteau, C.S., Vaino, D.C., Shah, M., Gopal, M., Davies, J., NIchols, D., Broden, J., *Field Relevance of a Suite of Rollover Tests to Real-World Crashes and Injuries.* Accident Analysis and Prevention, 2003. **35**: p. 103-110.
36. Cooperrider, N.K., Hammoud, S.A., Colwell, J., *Characteristics of Soil-Tripped Rollovers.* SAE 980022, 1998.
37. Orlowski, K.F., Bundorf, R. Thomas, Moffatt, Edward A., *Rollover Crash Tests - The Influence of Roof Strength on Injury Mechanics.* SAE 851734, 1985.
38. Liang, D.Y., Allen, W.R., Rosenthal, T.J., Chrstos, J.P., Nunez, P., *Tire Modeling for Off-Road Vehicle Simulation.* SAE 2004-01-2058, 2004.
39. Chrstos, J.P., Heydinger, G.J., *Evaluation of VDANL and VDM RoAD for Predicting the Vehicle Dynamics of a 1994 Ford Taurus.* SAE 970566, 1997.

40. Antoun, R.J., Hackert, P.B., O'Leary, M.C., Sitchin, A., *Vehicle Dynamic Handling Computer Simulation - Model Development, Correlation, and Application Using ADAMS.* SAE 860574, 1986.
41. Chace, M.A., Wielenga, T.J., *A Test and Simulation Process to Improve Rollover Resistance.* SAE 1999-01-0125, 1999.
42. Orlandea, N., Chace, M.A., *Simulation of a Vehicle Suspension with the ADAMS Computer Program.* SAE 770053, 1977.
43. Segal, D.J., Calspan Corporation, *Highway-Vehicle-Object Simulation Model: Engineering Manual - Validation, FHWA-RD-76-165*. 1976, FHWA.
44. Allen, R.W., Chrstos, J.P., Rosenthal, T.J., *A Vehicle Dynamics Tire Model for Both Pavement and Off-Road Conditions.* SAE 970559, 1997.
45. Gopal, M., Baron, K., Shah, M., *Simulation and Testing of a Suite of Field Relevant Rollovers.* SAE 2004-01-0335, 2004.
46. Steffan, H., Moser, A., *How to Use PC-Crash to Simulate Rollover Crashes.* SAE 2004-01-0341, 2004.
47. Cliff, W.E., Montgomery, D.T., *Validation of PC-Crash - A Momentum-Based Accident Reconstruction Program.* SAE 960885, 1996.
48. Bekker, M.G., *Introduction to Terrain-Vehicle Systems*. 1969, Ann Arbor: The University of Michigan Press.
49. Metz, L.D., *Dynamics of Four-Wheel-Steer Off-Highway Vehicles.* SAE 930765, 1993.

Chapter 3

Derivation of Low-Order Vehicle Dynamic Models

Automobiles are complex machinery, so modeling their dynamic characteristics and responses can be a difficult task. This task can be simplified by focusing on the purpose for modeling such behavior. If stability and safety are a main concern, most of the modeling can be focused on the chassis dynamics of a vehicle. By treating an automobile as a rigid body, Newton's laws of motion can be applied to derive equations of motion.

This chapter presents the derivations of low-order vehicle dynamic models derived using two different approaches. Terminology useful in model derivations will first be presented, followed by a 2-DOF linear model and then complexity will be added to account for roll dynamics and a roll inclusive model will also be derived.

3.1 Model Terminology

All derivations presented in this work will be derived in the SAE standard reference frame as shown in Figure 3.1.[1] This is a body-fixed coordinate system, meaning it is fixed to the body and moves with the vehicle.

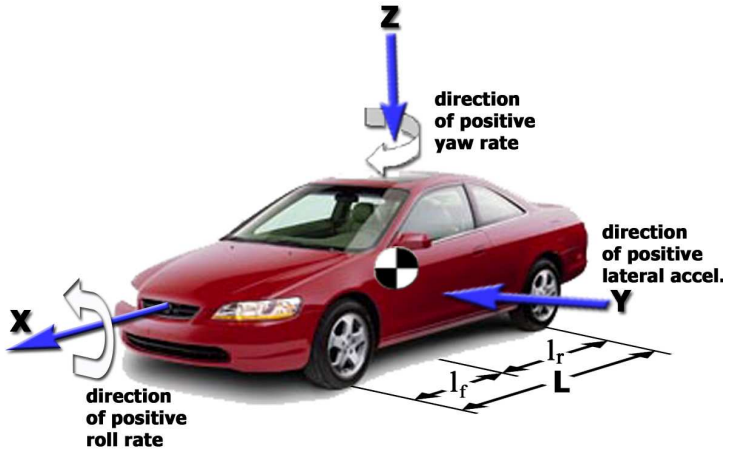

Fig. **3.1**: SAE Coordinate System

Common parameters such as speed and slip angles of the tires and vehicles are defined in Table **3.1**

Table **3.1**: Bicycle Model Parameters

Symbol	Parameter Definition
m	Mass of Vehicle
I_{zz}	Yaw Moment of Inertia
V_{CG}	Total Velocity of Vehicle CG
U	Forward Velocity of Vehicle
V	Lateral Velocity of Vehicle
β	Side-slip of Vehicle
α_f, α_r	Slip angle of front and rear tire
r	Yaw rate around Z-axis
δ_f	Front Steering Angle
F_f, F_r	Force generated at front and rear tire
a	Front Axle to CG distance
b	CG to Rear Axle distance

3.2 Two Degree of Freedom Linear Bicycle Model

A complex vehicle can be modeled as a relatively simple system by making a number of assumptions with the goal of simplicity in mind. Assumptions used to create the simple 2-DOF model include no roll, pitch or vertical motion, constant forward velocity, no aerodynamic forces, the chassis is a rigid body without suspension influences, that tire forces are linearly related to the tire slip angle, and the tires on either side of the vehicle produce the same force reactions. This last assumption makes it possible to lump together the wheels on the front and back axles to form one front and one real wheel, hence the name of the 2-DOF linear Bicycle Model [2-5]. Another common assumption used in the many of the derivations presented is that any changes in orientation angles are small enough such that the following equations hold:

$$\cos\theta \cong 1$$
$$\sin\theta \cong 0 \qquad \text{Eq } \mathbf{3.1}$$

The free-body diagram illustrating the forces and properties used to derive the 2-DOF linear model is shown in Figure **3.2**

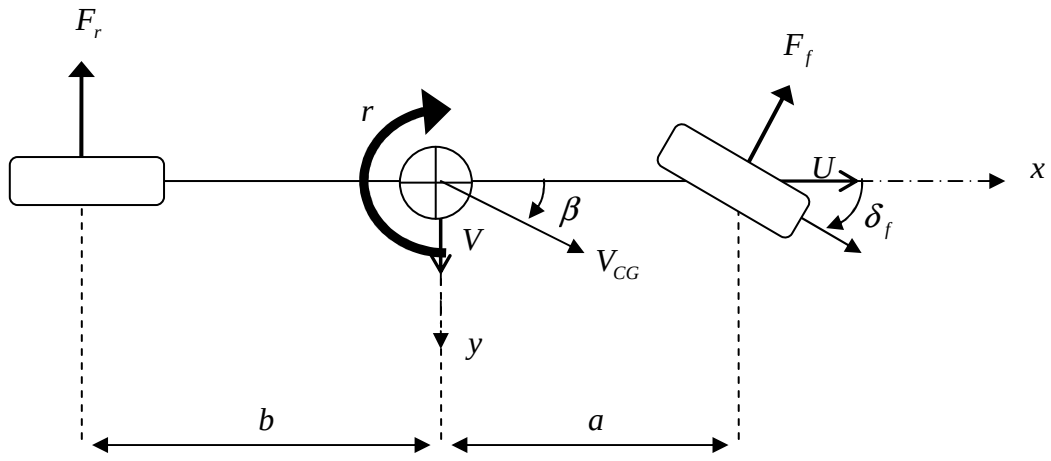

Fig. **3.2**: Free Body diagram 2-DOF

3.2.1 Newtonian Mechanics Derivation

The first approach for deriving a linear 2-DOF model utilizes Newton's second law of motion, $F = ma$. A vehicle experiences forces from a variety of inputs, the largest being the tire/ground interaction. Other forces include aerodynamic forces, changes in gravitational forces due to weight transfer and suspension forces, all of which will be assumed to be negligible. Summing forces in the y-direction produces Eq. **3.2.**

$$F_f + F_r = ma \qquad \text{Eq } \mathbf{3.2}$$

Recall that the equations of motion are derived from a body-fixed coordinate frame. Therefore, the accelerations are a combination of the directional acceleration and the rotational velocity of the vehicle as shown in Eq. **3.3.** [4]

$$\frac{dv}{dt}_{body} = \frac{dv}{dt}_{global} + \omega \times r \qquad \text{Eq } \mathbf{3.3}$$

Using the above equation, the governing equation for the vehicle body's lateral motion becomes Eq. **3.4.**

$$F_f + F_r = m\left(\dot{V} + rU\right) \qquad \text{Eq } \mathbf{3.4}$$

Summing the moments around the z-axis generates the governing equation for yaw motion, Eq. **3.5.**

$$F_f a - F_r b = I_{zz}\dot{r} \qquad \text{Eq } \mathbf{3.5}$$

For easy comparison between models presented throughout this work, all models will be presented in state-space form like Eq. **3.6**

$$\begin{aligned} \dot{x} &= Ax + Bu \\ y &= Cx + Du \end{aligned} \qquad \text{Eq } \mathbf{3.6}$$

In Eq. **3.6**, x represents the states of the system, such as lateral velocity, yaw rate and roll angle, u represents the inputs to the system, either the lateral forces at the tires or the front steering angle, and y represents the system outputs. Equations **3.4** and **3.5** combine

to form the governing equations known as the bicycle model, represented in state-space form in Eq. **3.7**

$$\begin{bmatrix} \dot{V} \\ \dot{r} \end{bmatrix} = \begin{bmatrix} 0 & -U \\ 0 & 0 \end{bmatrix} \begin{bmatrix} V \\ r \end{bmatrix} + \begin{bmatrix} \frac{1}{m} & \frac{1}{m} \\ \frac{a}{I_{zz}} & \frac{-b}{I_{zz}} \end{bmatrix} \begin{bmatrix} F_f \\ F_r \end{bmatrix} \qquad \text{Eq } \mathbf{3.7}$$

3.2.2 Lagrangian Mechanics Derivation

An alternative approach to Newton's second law of motion is to implement Lagrange's principles in the derivation process. Lagrange's principles use an energy approach to derive the governing equations of motion. Tabulating sources of kinetic (T) and potential (V) energy and inserting into the Lagrangian formulation shown in Eq. **3.8** for the generalized coordinate, q, will produce an equation of motion for the variable of interest [6].

$$\frac{d}{dt}\left(\frac{\partial T}{\partial \dot{q}}\right) - \frac{\partial T}{\partial q} + \frac{\partial V}{\partial q} = Q \qquad \text{Eq } \mathbf{3.8}$$

A vehicle with an assumed rigid chassis and no vertical motion does not store potential energy, but has three sources of kinetic energy, U, the forward velocity, V, the lateral velocity and r, the yaw rate. Forward velocity, U, is assumed to be constant, leaving two states to use in Lagrangian dynamics. Starting with lateral position, y, and applying Eq **3.6** yields Eq. **3.9**

$$\begin{gathered} \tfrac{d}{dt}\left(m\dot{y}\right) - 0 + 0 = F_f \cos\delta + F_r \\ my = F_f \cos\delta + F_r \end{gathered} \qquad \text{Eq } \mathbf{3.9}$$

Recall that Eq. **3.10**

$$\ddot{y} = \dot{V} + rU \qquad \text{Eq } \mathbf{3.10}$$

And considering only cases where the steering angle will be small, one can apply the small angle assumption to Eq **3.9** and insert Eq **3.10** to produce Eq. **3.11**

$$m\left(\dot{V}+rU\right)=F_f+F_r \qquad \text{Eq } \mathbf{3.11}$$

which is the same as Eq. **3.4** above.

The Lagrangian approach can then be applied to the state of yaw direction of the vehicle. This produces Eq. **3.12**

$$\frac{d}{dt}\left(I_{zz}r\right)-0+0=-F_r b+F_f a$$
$$I_{zz}\dot{r}=-F_r b+F_f a \qquad \text{Eq } \mathbf{3.12}$$

which is the same as Eq. **3.5** above.

3.3 Extension of Linear Model to Include Linear Tire Model

Governing equations of motion for both lateral velocity, V, and yaw rate, r, depend on tire forces generated in the lateral direction. To keep the above equations linear, a linear tire model was implemented. Tire forces were assumed to be proportional to the slip angle of each wheel as in Eq. **3.13**

$$F_f=C_f\alpha_f$$
$$F_r=C_r\alpha_r \qquad \text{Eq } \mathbf{3.13}$$

The slip angle of a wheel, α, is the difference in direction between the velocity vector of the wheel and the path of travel of the wheel as shown in Figure **3.3**

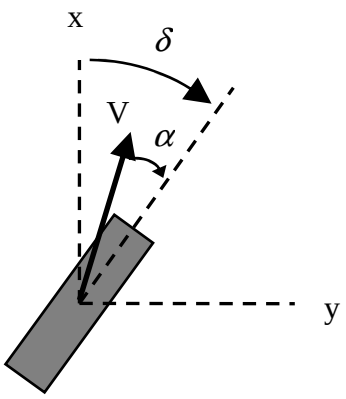

Fig. **3.3**: Slip Angle of Tire

This angle can be solved for by examining the force velocity components of the tire and the commanded steering input. The orientation of the tire is made up of the commanded steering input and the inverse tangent of the velocity components as depicted by ζ and shown in Figure **3.4**

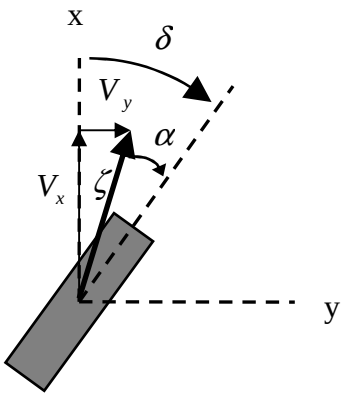

Fig. **3.4**: Tire Velocity Components

Using geometry and knowledge about the value of ζ, the value of the tire's slip angle can be calculated as in Eq. **3.14**.[2, 4, 5]

$$\alpha_f = \tan^{-1}\left(\frac{V_y}{V_x}\right) - \delta_f = \tan^{-1}\left(\frac{V + ar}{U}\right) - \delta_f$$
$$\alpha_r = \tan^{-1}\left(\frac{V_y}{V_x}\right) - \delta_r = \tan^{-1}\left(\frac{V - br}{U}\right) - \delta_r \qquad \text{Eq } \mathbf{3.14}$$

The small angle approximation can also be applied in this situation and the rear wheel steering input is usually set to zero since four wheel steer vehicles are very rare. Applying these assumptions yields Eq. **3.15**

$$\alpha_f = \frac{V + ar}{U} - \delta$$
$$\alpha_r = \frac{V - br}{U} \qquad \text{Eq } \mathbf{3.15}$$

Combining Eq **3.15** with Eq. **3.13** and inserting into Eq. **3.4** and Eq. **3.5** yields Eq. **3.16**

$$m\left(\dot{V} + rU\right) = C_f\left(\frac{V + ar}{U} - \delta\right) + C_r\left(\frac{V - br}{U}\right)$$
$$I_{zz}\dot{r} = C_f\left(\frac{V + ar}{U} - \delta\right)a - C_r\left(\frac{V - br}{U}\right)b \qquad \text{Eq } \mathbf{3.16}$$

Rearranging into standard state-space representation from Eq. **3.6** yields Eq. **3.17**

$$\begin{bmatrix}\dot{V}\\ \dot{r}\end{bmatrix} = \begin{bmatrix}\frac{C_f + C_r}{mU} & \frac{C_f a - C_r b}{mU} - U\\ \frac{C_f a - C_r b}{I_{zz}U} & \frac{C_f a^2 + C_r b^2}{I_{zz}U}\end{bmatrix}\begin{bmatrix}V\\ r\end{bmatrix} + \begin{bmatrix}\frac{-C_f}{m}\\ \frac{-C_f a}{I_{zz}}\end{bmatrix}[\delta] \qquad \text{Eq } \mathbf{3.17}$$

These equations will be used as a standard baseline model for comparing predicted vehicle motion to that measured during experimental testing.

3.4 Inclusion of Roll Dynamics

The linear bicycle model can be extended to capture roll motion. Inclusion of roll dynamics introduces another state of vehicle motion, roll angle. The three equations of

motion governing vehicle motion and accounting for roll dynamics will again be derived in both Newtonian and Lagrangian approaches. A new aspect introduced by including roll dynamics is the separation of the mass of the vehicle into sprung and unsprung parts. The distinction arises because the sprung mass is supported by the suspension and stiffness of the vehicle, modeled as a spring and damper, as shown in Figure **3.5**

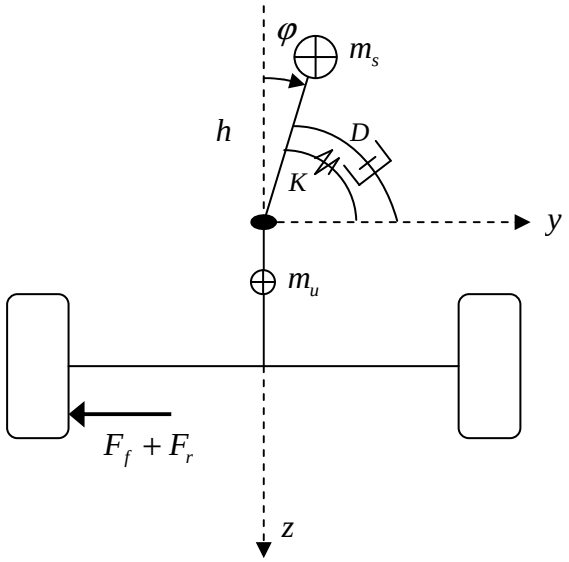

Fig. **3.5**: Free Body Diagram 3 DOF (view from behind)

There are some additional vehicle parameters needed in the derivation of a roll inclusive model. Those parameters are listed in Table **3.2**

Table **3.2**: Vehicle Parameters needed in Roll Inclusive Model

Symbol	Vehicle Parameter
m_s	Sprung Mass of Vehicle
m_u	Unsprung Mass of Vehicle
I_{xx}	Roll Moment of Inertia
ϕ	Roll Angle
h	Roll axis to CG Height
K	Suspension Spring Stiffness
D	Suspension Damping Coefficient
g	Gravity

3.4.1 Newtonian Mechanics Derivation to Include Roll

Similar to the 2-DOF linear model, a summation of forces in the lateral direction gives the governing equation in the y direction,

$$\begin{aligned}\Sigma F_y &= ma_y \\ F_f + F_r &= m_u\left(\dot{V}+Ur\right)+m_s\left(\dot{V}+Ur+h\ddot{\phi}\right) \\ F_f + F_r &= m\left(\dot{V}+Ur\right)+m_s h\ddot{\phi}\end{aligned} \qquad \text{Eq } \mathbf{3.18}$$

and around the Z-axis

$$\begin{aligned}\Sigma M_z &= I_{zz}\dot{r} \\ aF_f - bF_r &= I_{zz}\dot{r}\end{aligned} \qquad \text{Eq } \mathbf{3.19}$$

and now also around the X-axis

$$\begin{aligned}\Sigma M_x &= I_{xx}\ddot{\phi} \\ -K\phi - D\dot{\phi} - m_s h\left(\dot{V}+Ur\right)+m_s gh\phi &= \left(I_{xx}+m_s h^2\right)\ddot{\phi}\end{aligned} \qquad \text{Eq } \mathbf{3.20}$$

Combining Eq. **3.18**, Eq. **3.19** and Eq. **3.20** yields three linear equations that govern vehicle motion. All three are summarized in Eq. **3.21**.

$$\begin{aligned}m\left(\dot{V}+Ur\right)+m_s h\ddot{\phi} &= F_f + F_r \\ I_{zz}\dot{r} &= aF_f - bF_r \\ \left(I_{xx}+m_s h^2\right)\ddot{\phi} &= -m_s h\left(\dot{V}+Ur\right)-D\dot{\phi}+\left(m_s gh-K\right)\phi\end{aligned} \qquad \text{Eq } \mathbf{3.21}$$

And can be represented in state-space form as Eq. **3.22**

$$\begin{bmatrix}\dot{V}\\ \dot{r}\\ \dot{\phi}\\ \ddot{\phi}\end{bmatrix} = \begin{bmatrix} \frac{C_f+C_r}{UJ_1} & \frac{m_s^2h^2U}{J_2}+\frac{aC_f-bC_r}{UJ_1} & -\frac{U}{J_1} & \frac{m_sh\left(m_sgh-K\right)}{J_2} & \frac{m_shD}{J_2} \\ \frac{aC_f-bC_r}{UI_{zz}} & \frac{a^2C_f+b^2C_r}{UI_{zz}} & 0 & 0 & \\ 0 & 0 & 0 & 1 & \\ \frac{-m_sh\left(C_f-C_r\right)}{mUJ_2} & \frac{m_sh\left(aC_f-bC_r\right)}{mUJ_2} & & \frac{m_sgh-K}{J_2} & \frac{-D}{J_2} \end{bmatrix} \begin{bmatrix}V\\ r\\ \phi\\ \dot{\phi}\end{bmatrix} + \begin{bmatrix}\frac{-C_f}{J_1}\\ \frac{-aC_f}{I_{zz}}\\ 0\\ \frac{C_fm_sh}{mJ_2}\end{bmatrix}[\delta] \qquad \text{Eq } \mathbf{3.22}$$

$$J_1 = m - \frac{m_s^2h^2}{I_{xx}+m_sh^2} \qquad J_2 = I_{xx}+m_sh^2-\frac{m_s^2h^2}{m}$$

3.4.2 Lagrangian Dynamics Derivation to Include Roll

Using the Lagrangian dynamics approach will yield the same three equations derived above by also using the state of roll angle.

Applying the Lagrangian approach to the state of lateral position yields Eq. **3.23**

$$\begin{aligned} &\frac{d}{dt}\left(m_s\dot{y}+m_sh\dot{\phi}\right)-0+0=F_f+F_r \\ &m_s\ddot{y}+m_sh\ddot{\phi}=F_f+F_r \\ &m_s\left(\dot{V}+Ur\right)+m_sh\ddot{\phi}=F_f+F_r \end{aligned} \qquad \text{Eq } \mathbf{3.23}$$

Moving on to yaw rate produces the same equation regardless of the added inclusion of roll dynamics.

$$\begin{aligned} &\frac{d}{dt}\left(I_{zz}r\right)-0+0=aF_f-bF_r \\ &I_{zz}\dot{r}=aF_f-bF_r \end{aligned} \qquad \text{Eq } \mathbf{3.24}$$

And now introducing the state of roll angle produces Eq. **3.25**

$$\begin{aligned} &\frac{d}{dt}\left(I_{xx}\dot{\phi}+m_sh\dot{y}+m_sh^2\dot{\phi}\right)-0-m_sgh\phi+K\phi=-D\dot{\phi} \\ &I_{xx}\ddot{\phi}+m_sh\left(\ddot{y}+h\ddot{\phi}\right)-m_sgh\phi+K\phi=-D\dot{\phi} \\ &I_{xx}\ddot{\phi}=-D\dot{\phi}-K\phi-m_sh\left(\dot{V}+Ur+h\ddot{\phi}\right)+m_sgh\phi \end{aligned} \qquad \text{Eq } \mathbf{3.25}$$

Rearranging and combining Eq. **3.23**, Eq. **3.24** and Eq. **3.25** produces the same three equations that govern vehicle motion obtained from using Newtonian mechanics and summarized in Eq. **3.22**.

1. *SAE J670e 1976*. Vehicle Dynamics Technology. 1976, Warrendale, PA: Society of Automotive Engineers, Inc.
2. Bundorf, R.T., *A Primer on Vehicle Directional Control*. 1968, Warren: General Motors Technical Center: Michigan Engineering Publication.
3. Gillespie, T.D., *Fundamentals of Vehicle Dynamics*. 1992, Warrendale, PA: Society of Automotive Engineers, Inc.
4. Karnopp, D., *Vehicle Stability*. 2004, New York: Marcel Dekker, Inc.
5. Pacejka, H.B., *Tire and Vehicle Dynamics*. 2nd ed. 2006, Warrendale, PA: Society of Automotive Engineers, Inc,.
6. Ginsberg, J.H., *Advanced Engineering Dynamics*. 2nd ed. 1998, New York: Cambridge University Press.

Chapter 4

Validation of Vehicle Dynamics Models

4.1 Experimental Testing

Experimental tests were performed at the Pennsylvania Transportation Institute's test track facility outside State College, Pennsylvania to analyze the ability of the previously derived models to describe vehicle chassis and roll behavior. The measured data allowed for some unknown model parameters, such as tire cornering stiffness to be determined during the validation process. Discrepancies between model prediction and measured data suggested the need for further exploration of vehicle dynamics.

4.1.1 Data Acquisition System

A 5-door 1992 Mercury Tracer was utilized during the experimental testing. The Tracer's steering column was instrumented with two string potentiometers to measure steering input. This was calibrated using tire slip plates to relate the potentiometer voltage reading to tire angle. The Tracer was also instrumented with an integrated differential GPS and inertial measurement unit. Details of the integration process and installation of the data acquisition system can be found in Ryan Martini's Master's Thesis [1].

The data acquisition system is highly accurate, producing resolutions of 2 cm in position, and angle accuracies of 0.013° for roll and pitch and 0.04° of yaw [1]. Available outputs from the system include position, speed, and accelerations in the three principal directions and headings about all three axes.

4.1.2 Testing Procedures

A variety of tests were performed to allow for multiple comparisons between model predictions and experimental data. Each testing session commenced with three straight line tests along a laser aligned rail on the track surface to capture any offsets due to variations in mounting of the IMU, or drift in the string potentiometers that measured steering input. Testing maneuvers included single lane changes, step steer inputs, steady-state driving around circles of two different sizes and a series of sine waves to produce a swept sine view of the vehicle's response. The swept sine data was generated by inputting sine waves of constant frequency as steering inputs by the use of an electronic metronome, and measuring the vehicle's response. This was repeated using sine waves of frequencies ranging from 0.1667 Hz to 3.5 Hz. To check for linearity of the system, two complete swept sine tests were performed, one for steering inputs of small amplitude, and one for large amplitude. The large amplitude sine wave involved a hand wheel rotation varying from 2 o'clock to 10 o'clock and the small amplitude steering input varied from 1 o'clock to 11 o'clock.

4.1.3 Vehicle Parameters

The bicycle model contains vehicle parameters that can be easily measured, except for the front and rear cornering stiffnesses of the tires [2]. The location of the roll axis was found by videotaping the front and rear bumper of the vehicle while the vehicle was subjected to a rocking motion. From the videotape, the center of rotation was determined at each bumper, and then at the vehicle CG using similar triangles. The vehicle parameters used in the bicycle and roll model are listed in Table **4.1**

Table 4.1: Vehicle Parameters

Variable	Value	Parameter
m	1030 kg	Vehicle Mass
m_s	824 kg	Vehicle Sprung Mass
W_f	6339 N	Weight Front Axle
W_r	3781 N	Weight Rear Axle
a	0.93 m	Front Axle to CG
b	1.56 m	CG to Rear Axle
L	2.49 m	Vehicle Wheelbase
h	0.26 m	Roll Axis to CG
I_{zz}	1850 kg m^2	Yaw Moment of Inertia
I_{yy}	1705 kg m^2	Pitch Moment of Inertia
I_{xx}	375 kg m^2	Roll Moment of Inertia
I_{xz}	72 kg m^2	Moment of Inertia XZ-plane

4.2 Validation of Dynamic Models

Vehicle testing was done under both transient and steady-state conditions, but for the purpose of validating vehicle models to be used in transient situations, the transient maneuvers are of higher interest for they include more dynamic behavior. Therefore, validation efforts focused on data from the swept sine test. The results are represented in the frequency domain where the top plot relates the magnitude of the output, either lateral velocity, yaw rate or roll, to the magnitude of the input, in this case, steering angle. The bottom plot relates the phase or time lag between the input and output of the system. Figure 4.1, Figure 4.2 and Figure 4.3 show the frequency domain responses for lateral velocity, yaw rate and roll angle for both the large and small amplitude sine waves.

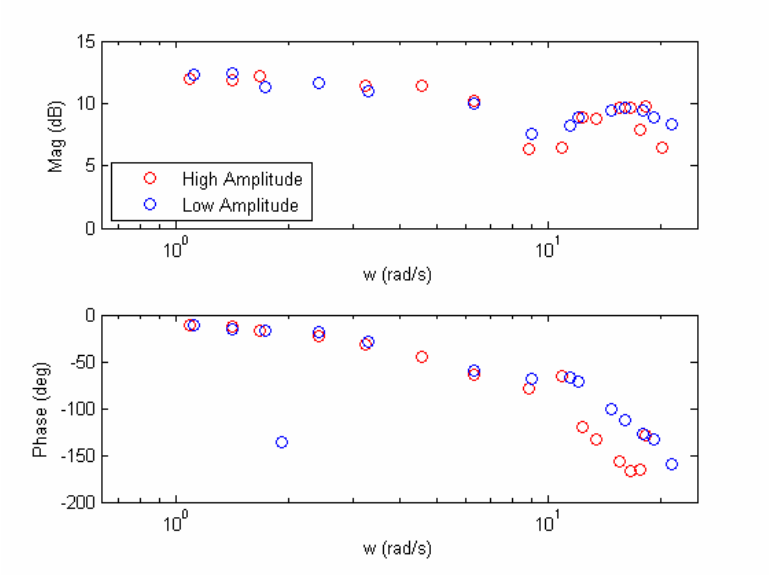

Fig. **4.1**: Frequency Response of Lateral Velocity

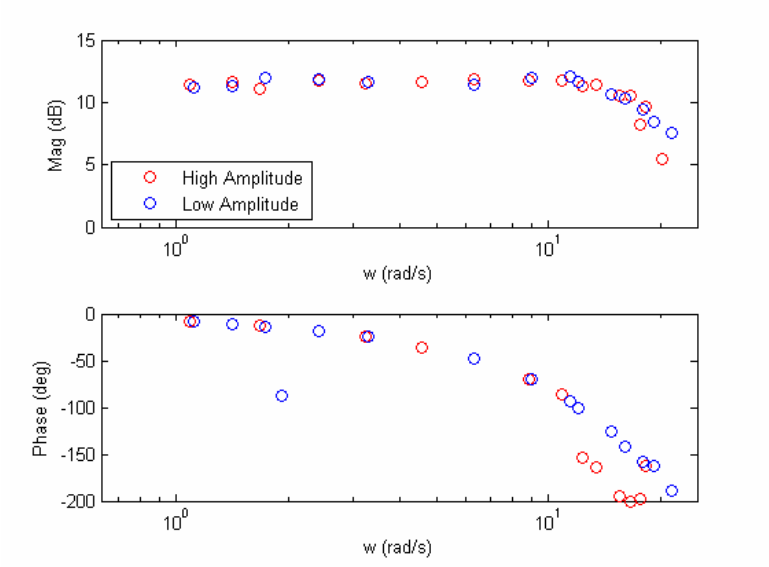

Fig. **4.2**: Frequency Response of Yaw Rate

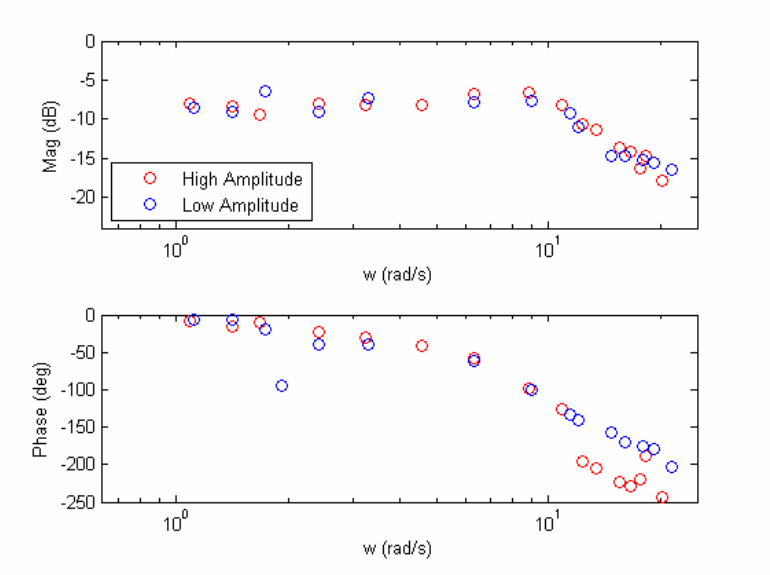

Fig. **4.3**: Frequency Response of Roll Angle

As previously mentioned, the linear bicycle model only has two parameters that are hard to measure, the front and rear cornering stiffnesses. Therefore, the validation process will first concentrate on the 2-DOF model to determine the cornering stiffnesses before adding complexity and additional parameters to the model.

The method to find the cornering stiffnesses utilized steady-state data since it should be least influenced by higher order dynamics. The data was analyzed by looking at the gains between the input of steering to the output under consideration, either lateral velocity or yaw rate. The system gain during a sine wave input is referred to as the DC gain of the system and is usually seen by a flat trend in the response at very low frequencies on a frequency response plot, such as Figure **4.1** Attempts were made to match the DC gains measured at low frequencies with calculated gains from the dynamic model.

The DC gains for the vehicle response can be calculated using the state space representation of the bicycle model in Eq. **4.1**

$$G = D - CA^{-1}B \qquad \text{Eq } \mathbf{4.1}$$

In the bicycle model derived in Chapter 3, the C matrix is the identity matrix and the D matrix is null since the outputs of interest are the states of the system. Substituting the A and B matrix of the bicycle model from Eq. **3.16**, and simplifying, the lateral velocity gain is Eq. **4.2**

$$G_v = \frac{U\left(C_f C_r bL + C_f amU^2\right)}{C_f C_r\left(a^2 + b^2 + 2ab\right) + mU^2\left(aC_f - bC_r\right)} \qquad \text{Eq } \mathbf{4.2}$$

Similarly, for yaw rate Eq. **4.3**

$$G_r = \frac{UC_f C_r L}{C_f C_r\left(a^2 + b^2 + 2ab\right) + mU^2\left(aC_f - bC_r\right)} \qquad \text{Eq } \mathbf{4.3}$$

Numerical values were obtained by averaging the high and low amplitude frequency responses, which yielded a value of $G_v = 4.0546\,\text{m/s}$ lateral velocity per radian of steering input and $G_r = 3.6830\,\text{rad/sec}$ yaw rate per radian of steering input. Combining Eq. **4.2** and Eq. **4.3** and rearranging for front and rear cornering stiffness yields Eq. **4.4**

$$C_r = \frac{amU^2 G_r}{\left(G_v - bG_r\right)L} = -91{,}235\,\frac{\text{N}}{\text{rad}}$$
$$C_f = \frac{-U^2 mG_r C_r b}{C_r UL - G_r C_r L^2 - U^2 mG_r a} = -87{,}251\,\frac{\text{N}}{\text{rad}} \qquad \text{Eq } \mathbf{4.4}$$

These cornering stiffness values generate the fits shown in Figure **4.4** and Figure **4.5**.

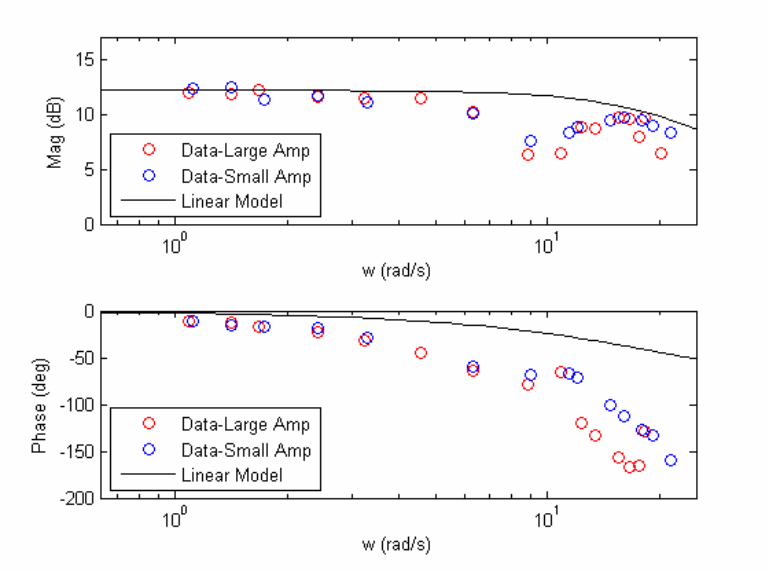

Fig. **4.4**: Model Prediction of Lateral Velocity

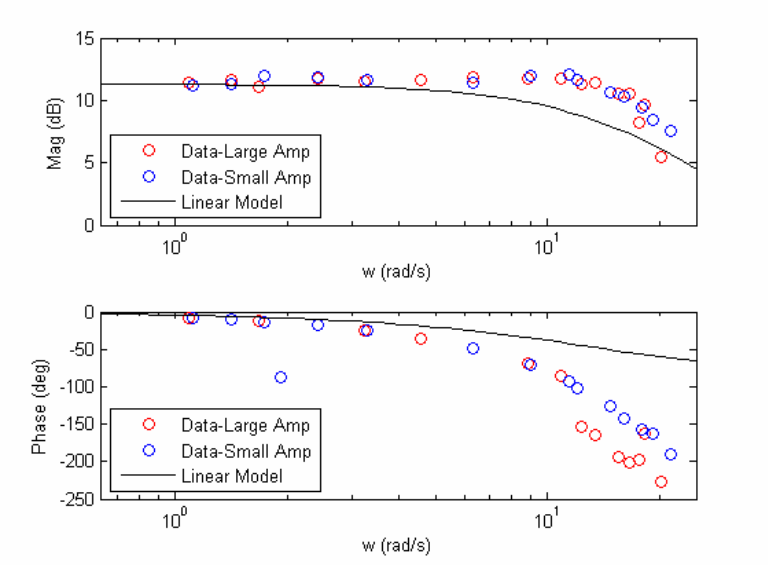

Fig. **4.5**: Model Prediction of Yaw Rate

It became obvious from the model comparison that the simple bicycle model is not fully capturing all the dynamics of the vehicle, especially at and above 1 Hz.

Applying the cornering stiffness values obtained from matching the frequency response data to steady-state situations yielded some discrepancies, as can be seen in Figure **4.6**

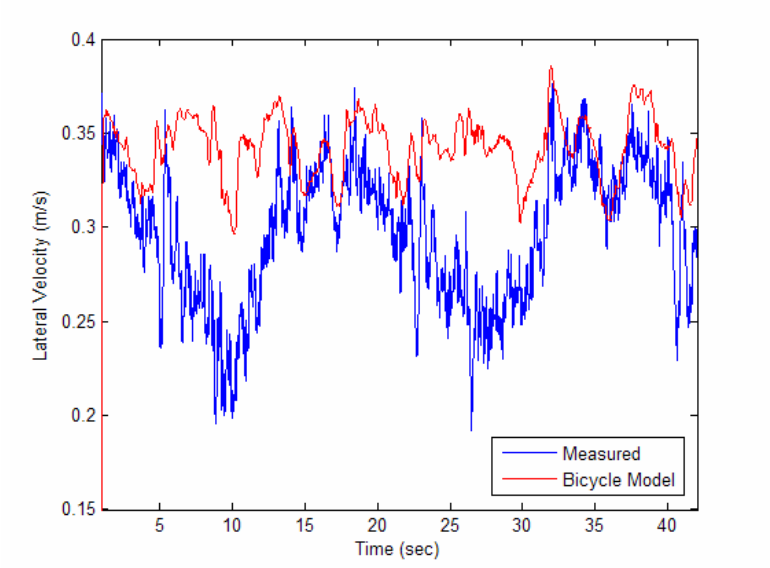

Fig. **4.6**: Lateral Velocity in 25 mph Steady-State Circle

A similar offset can be seen the in the yaw rate data as well. By parametrically fitting the cornering stiffness, values can be found so that the model more accurately predicts the measured response during steady state circles, but these values do not result in a good correlation to measured swept sine data. There are several differences between the dynamics of a steady-state and transient maneuver, such as tire lag and roll influences. These were investigated further in attempts to modify the models to better predict vehicular behavior.

4.2.1 Lag in Tire Force Generation

One common modification to the bicycle model used to compensate for transient maneuvers is the inclusion of the tire lag phenomenon. This phenomenon has been implemented by many researchers to capture the lag in force generation seen during

transient maneuvers [3, 4]. Lateral force on the tire is a result of both the deformation of the tire and the scrubbing of the tire against the pavement. The linear tire model equates lateral force to slip angle, but the resulting deformation after a change in tire angle is not instantaneous. This delay in force generation is commonly referred to as tire lag.

Tire lag is most commonly modeled as a simple 1-DOF time delay system with a time constant of $\tau = \frac{\sigma}{U}$ where σ is the relaxation length of the tire, referring to the rotational distance required for the tire deformation to reach steady state conditions. Therefore, the tire force at any instantaneous moment is a result of the steady state force expected under given conditions minus a partial amount based upon the relaxation length of the tire, the current speed and current tire force as seen in Eq. **4.5**

$$F = F_{ss} - \frac{\sigma}{U}\dot{F} \qquad \text{Eq } \mathbf{4.5}$$

Inclusion of tire lag into the linear bicycle model creates two additional states, tire force at the front and rear tires. Adding these states to the bicycle model and rearranging into state space representation yields Eq. **4.6**

$$\begin{bmatrix} \dot{V} \\ \dot{r} \\ \dot{F}_f \\ \dot{F}_r \end{bmatrix} = \begin{bmatrix} 0 & -U & \frac{1}{m} & \frac{1}{m} \\ 0 & 0 & \frac{a}{I_{zz}} & \frac{-b}{I_{zz}} \\ \frac{C_f}{\sigma} & \frac{aC_f}{\sigma} & -\frac{U}{\sigma} & 0 \\ \frac{C_r}{\sigma} & -\frac{bC_r}{\sigma} & 0 & -\frac{U}{\sigma} \end{bmatrix} \begin{bmatrix} V \\ r \\ F_f \\ F_r \end{bmatrix} + \begin{bmatrix} 0 \\ 0 \\ -\frac{C_f}{\sigma} \\ 0 \end{bmatrix} [\delta] \qquad \text{Eq } \mathbf{4.6}$$

While the inclusion of tire lag does not affect the model correlation in steady state maneuvers, the benefits of adding tire lag are evident when examining the frequency response representation of transient maneuvers. The magnitude plots for both lateral velocity and yaw rate show a slight peak in the measured data around 1 Hz, and the addition of tire lag helps capture this trend. The value of sigma was determined by parametric variation until a good correlation was obtained when $\sigma = 0.7$. Figure **4.7** and

Figure **4.8** show the comparison of the linear bicycle model with and without the addition of tire lag.

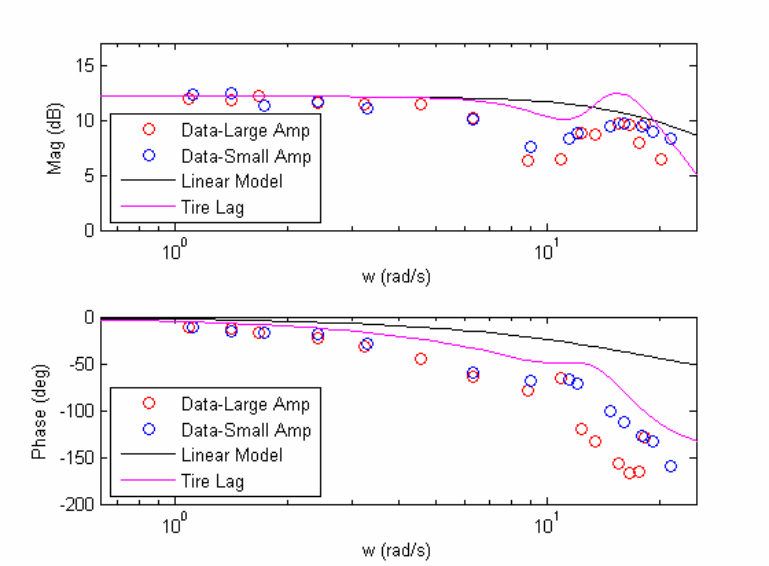

Fig. **4.7**: Lateral Velocity Frequency Response

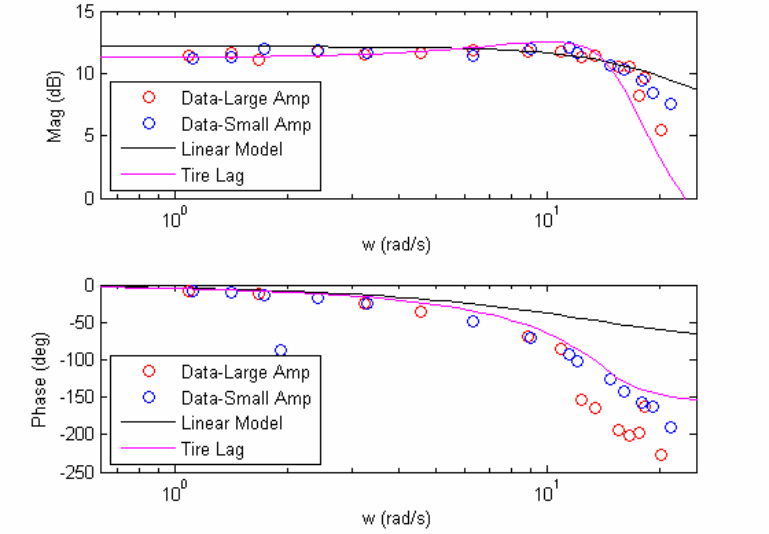

Fig. **4.8**: Yaw Rate Frequency Response

4.2.2 Roll Influence

Vehicle response measured during a steady-state circle will include roll influences, while transient maneuvers with low excitation levels may not. To address this discrepancy, a further investigation into cornering stiffness values was started. Using data from steady-state circle tests, the slip angle of the front and rear tire was calculated, as was the force at each tire required to keep the vehicle moving in a steady-state circle. The slip angle of each tire was plotted against the force at its respective axle as shown in Figure **4.9**

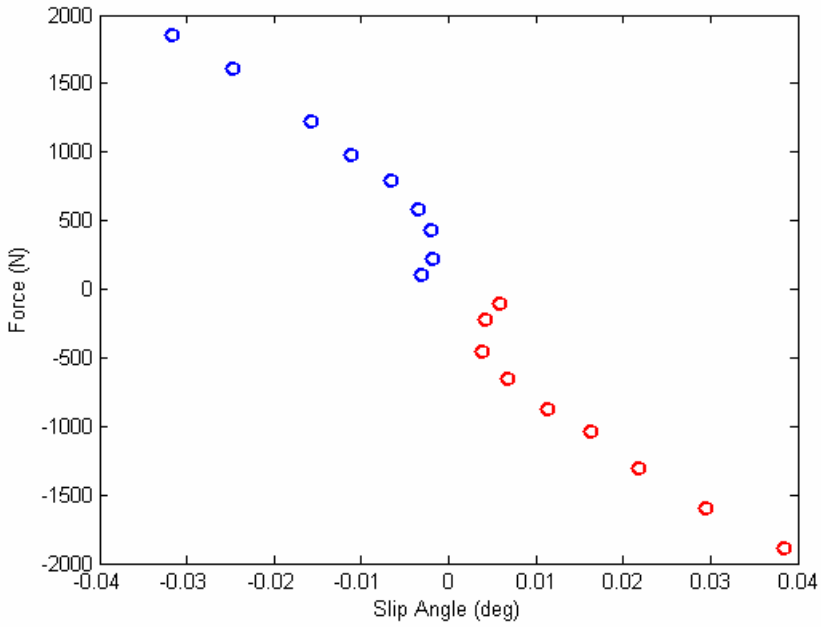

Fig. **4.9**: Rear Tire Slip Angle vs. Rear Axle Lateral Force

The data shows a linear relationship throughout most of the range tested which is the basis of a linear tire model, but at very low slip angles, the resulting curve produces unpredicted behavior. When plotting the force versus roll angle as shown in Figure **4.10** , a linear plot is produced for all values tested.

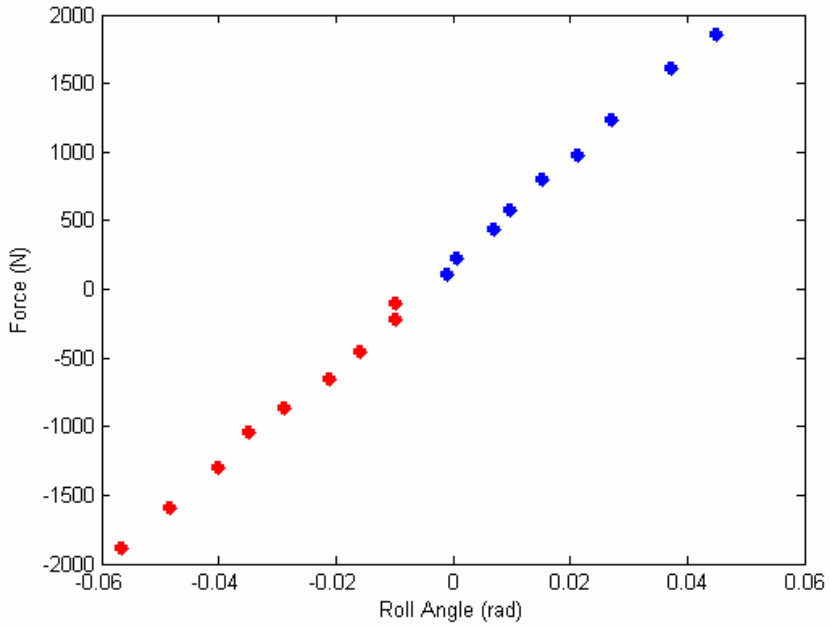

Fig. **4.10**: Vehicle Roll Angle vs. Rear Axle Lateral Force

With these observations, it was inferred that another mechanism to produce tire force was occurring during steady turning.

4.2.3 Camber Influence

An influence from roll motion on tire force generation was suspected during steady-state cornering, so the system gains were analyzed to help determine the quantitative effect of vehicle roll on the generated tire forces. Equations were derived from steady-state geometry to predict steering angle, lateral velocity and yaw rate. From these equations, the gains were numerically calculated and compared to values obtained from experimental data. This process is described below.

To account for the additional force generation source assumed to be from wheel camber, the bicycle model was initially modified to include a modified tire model based on tire slip angle and tire camber angle as in Eq. **4.7**

$$F = C\alpha + C_{\phi}\phi_{w} \qquad \text{Eq } \mathbf{4.7}$$

where ϕ_w is the camber angle of the tire and C_ϕ is the proportionality constant relating tire camber to generated lateral tire force. The camber angle of the wheel is proportionally related to the roll angle of the vehicle by a constant S as Eq. **4.8**

$$\phi_w = S\phi_v \qquad \text{Eq } \mathbf{4.8}$$

Solving Eq. **3.19** in steady state conditions for roll angle and substituting into Eq. **4.8** yields Eq. **4.9**

$$\phi_w = S\frac{m_s h}{K}\frac{U^2}{R} \qquad \text{Eq } \mathbf{4.9}$$

Recalling Eq. **3.4** and Eq. **3.5**, the tire forces during steady state circles can be written as Eq. **4.10** [3, 5]

$$\begin{aligned} F_f &= \frac{b}{L}\frac{mU^2}{R} \\ F_r &= \frac{a}{L}\frac{mU^2}{R} \end{aligned} \qquad \text{Eq } \mathbf{4.10}$$

Solving Eq. **4.7**, Eq. **4.9** and Eq. **4.10** for the front and rear slip angles while navigating a circle under steady-state conditions gives Eq. **4.11**

$$\begin{aligned} \alpha_f &= \frac{1}{C_f}\left[\frac{b}{L}\frac{mU^2}{R} - \frac{C_{\phi f} m_s h}{K} S_f \frac{U^2}{R}\right] \\ \alpha_r &= \frac{1}{C_r}\left[\frac{a}{L}\frac{mU^2}{R} - \frac{C_{\phi r} m_s h}{K} S_r \frac{U^2}{R}\right] \end{aligned} \qquad \text{Eq } \mathbf{4.11}$$

At steady state, the steering is geometrically dependent on the size of the turning circle and the front and rear slip angles[3, 5, 6] as written in Eq. **4.12**

$$\delta = \frac{L}{R} + \alpha_f - \alpha_r \qquad \text{Eq } \mathbf{4.12}$$

which can then be rewritten using Eq. **4.11** as Eq. **4.13**

$$\delta = \frac{L}{R} + \frac{1}{C_f}\left[\frac{b}{L}\frac{mU^2}{R} - C_f^*\frac{U^2}{R}\right] - \frac{1}{C_r}\left[\frac{a}{L}\frac{mU^2}{R} - C_r^*\frac{U^2}{R}\right] \qquad \text{Eq } \mathbf{4.13}$$

where Eq. **4.14**

$$C_f^* = \frac{C_{\phi f} m_s h}{K} S_f$$
$$C_r^* = \frac{C_{\phi f} m_s h}{K} S_r \qquad \text{Eq } \mathbf{4.14}$$

for simplicity.

The yaw rate and lateral velocity of a vehicle at steady sate conditions reduce to simple equations:

$$r = \frac{U}{R} \qquad \text{Eq } \mathbf{4.15}$$

$$V = U\beta = U\left(\frac{b}{R} + \alpha_r\right) \qquad \text{Eq } \mathbf{4.16}$$

Using Eq **3.13**, Eq. **3.15** and Eq **3.16**, the steady-state gains for lateral velocity and yaw rate around a circle of constant radius can be written as Eq. **4.17** and Eq. **4.18**

$$\frac{r}{\delta_f}_{circle} = \frac{\frac{U}{R}}{\frac{L}{R} + \frac{1}{C_f}\left[\frac{b}{L}\frac{mU^2}{R} - C_f^*\frac{U^2}{R}\right] - \frac{1}{C_r}\left[\frac{a}{L}\frac{mU^2}{R} - C_r^*\frac{U^2}{R}\right]} \qquad \text{Eq } \mathbf{4.17}$$

$$\frac{V}{\delta_f}_{circle} = \frac{U\left(\frac{b}{R} + \alpha_r\right)}{\frac{L}{R} + \frac{1}{C_f}\left[\frac{b}{L}\frac{mU^2}{R} - C_f^*\frac{U^2}{R}\right] - \frac{1}{C_r}\left[\frac{a}{L}\frac{mU^2}{R} - C_r^*\frac{U^2}{R}\right]} \qquad \text{Eq } \mathbf{4.18}$$

The system gains during circle maneuvers can be obtained by averaging the inputs and outputs of interest. Averaging the steering input and measured lateral velocity and yaw rate during steady-state circles gave gain values of $G_v = 3.3721$ m/s lateral velocity per radian of steering input and $G_r = 3.7531$ rad/sec of yaw rate per radian of steering input.

Using the gain values obtained from the steady-state cornering data, and the values of cornering stiffness calculated during low frequency sinewave maneuvers, the two remaining unknowns, C_f^* and C_r^* were determined to be $C_f^* = -119.5\,\text{kg}$ and $C_r^* = -169.4\,\text{kg}$.

Including the effects of tire camber produce model predictions that more closely correlate with the experimental results, as can be seen in Figure **4.11**

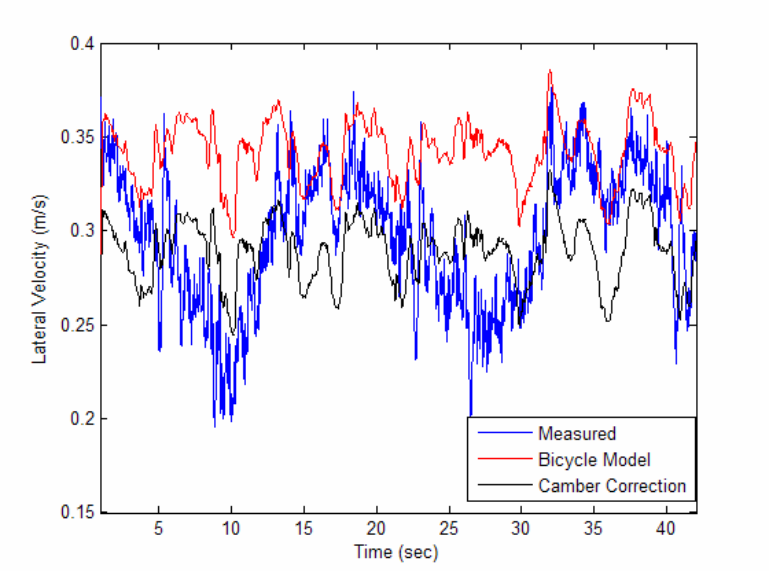

Fig. **4.11**: Lateral Velocity with Camber Correction

4.2.4 Roll Dynamic Validation

The 2-DOF linear model with the inclusion of both tire lag and a camber correction term produced good correlations between the measured data and the predicted vehicle response, thus providing a solid foundation for the addition of roll dynamics. The roll model, originally presented in Eq. **3.20** was updated to include the tire lag and camber correction term. The updated model is presented in state-space form in Eq. **4.19**

$$\begin{bmatrix} V \\ r \\ \phi \\ \dot{\phi} \\ F_f \\ F_r \end{bmatrix} = \begin{bmatrix} 0 & -U & \frac{-m_s h(m_s g h - K)}{I_1} & \frac{m_s h D}{I_1} & \frac{I_{xx} + m_s h^2}{I_1} & \frac{I_{xx} + m_s h^2}{I_1} \\ 0 & 0 & 0 & 0 & \frac{a}{I_{zz}} & \frac{-b}{I_{zz}} \\ 0 & 0 & 0 & 1 & 0 & 0 \\ 0 & 0 & \frac{m(m_s g h - K)}{I_1} & \frac{mD}{I_1} & \frac{-m_s h}{I_1} & \frac{-m_s h}{I_1} \\ \frac{C_f}{\sigma} & \frac{aC_f}{\sigma} & \frac{C_{rf} U}{h\sigma} & 0 & \frac{-U}{\sigma} & 0 \\ \frac{C_r}{\sigma} & \frac{-bC_r}{\sigma} & 0 & \frac{C_{rr} U}{h\sigma} & 0 & \frac{-U}{\sigma} \end{bmatrix} \begin{bmatrix} V \\ r \\ \phi \\ \dot{\phi} \\ F_f \\ F_r \end{bmatrix} + \begin{bmatrix} 0 \\ 0 \\ 0 \\ 0 \\ \frac{-C_f U}{\sigma} \\ 0 \end{bmatrix} [\delta] \qquad \text{Eq 4.19}$$

$$I_1 = m I_{xx} + m m_s h^2 - m_s^2 h^2$$

Two new parameters introduced in the roll dynamic model, K and D, are not easily measured, so were parametrically fit. The resulting model fits are shown in Figure **4.12**, Figure **4.13** and Figure **4.14**.

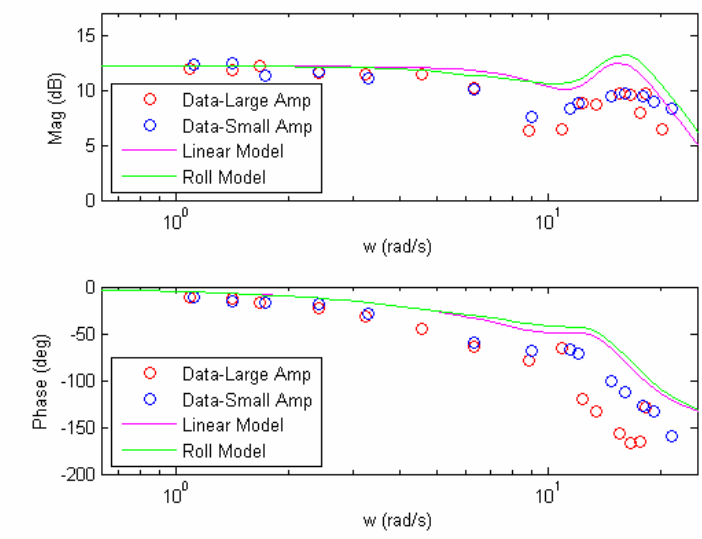

Fig. **4.12**: Lateral Velocity Frequency Response

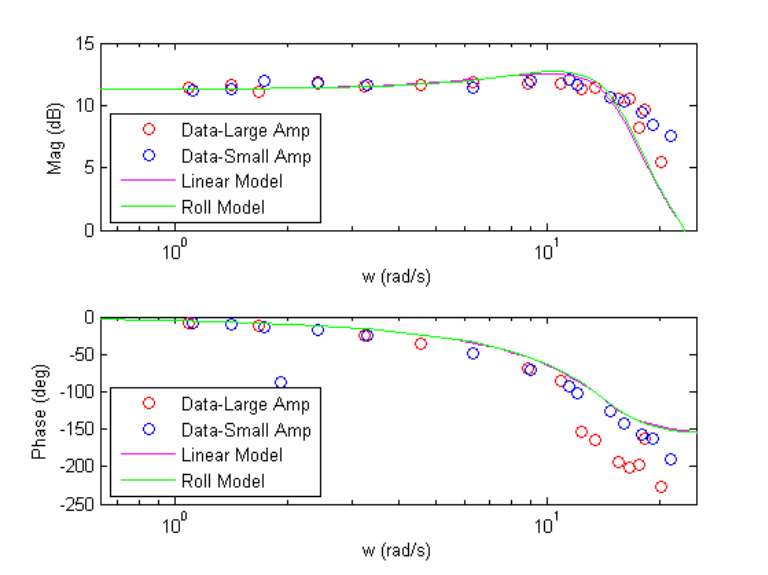

Fig. **4.13**: Yaw Rate Frequency Response

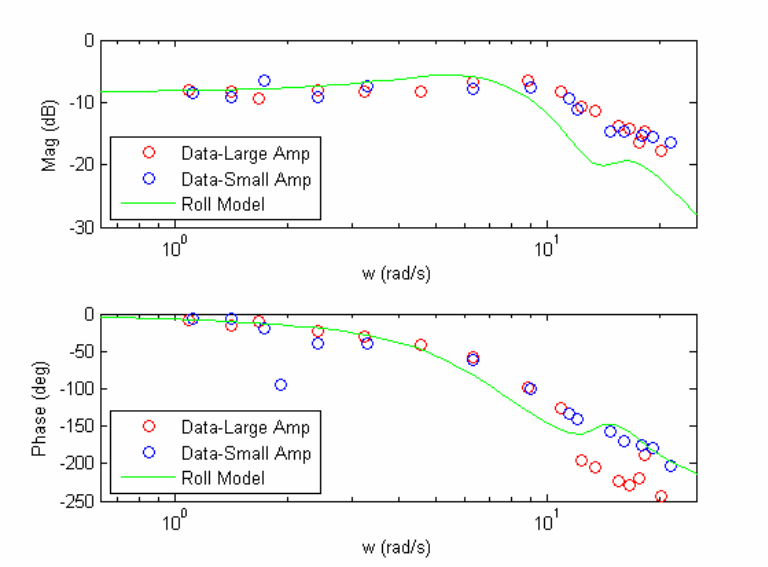

Fig. **4.14**: Roll Angle Frequency Response

The addition of roll dynamics improves the model prediction at higher frequencies, thus proving to be more suitable model for modeling avoidance maneuvers.

Emergency lane change maneuvers were also performed during the validation process. The roll inclusive model proved to be very capable of predicting vehicular response during such maneuvers. The vehicle response and model prediction are shown in Figure **4.15** Figure **4.16** and Figure **4.17**

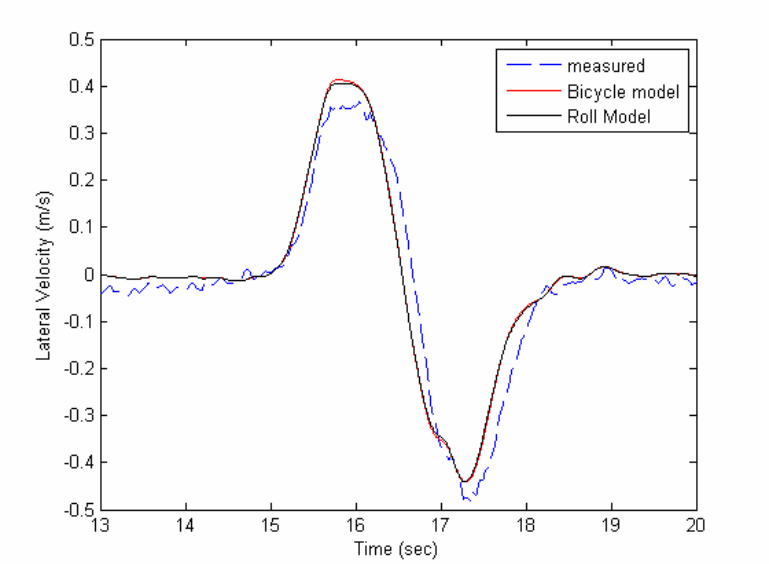

Fig. **4.15**: Lateral Velocity Response – Lane Change

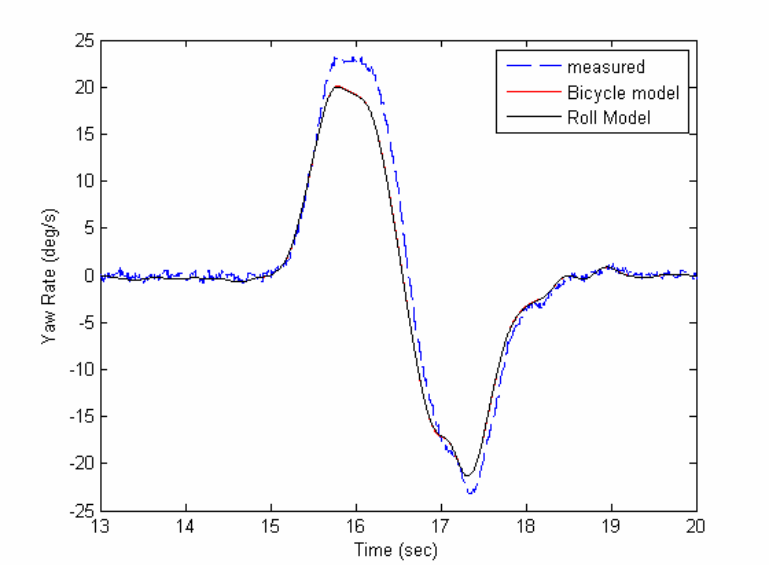

Fig. **4.16**: Yaw Rate Response – Lane Change

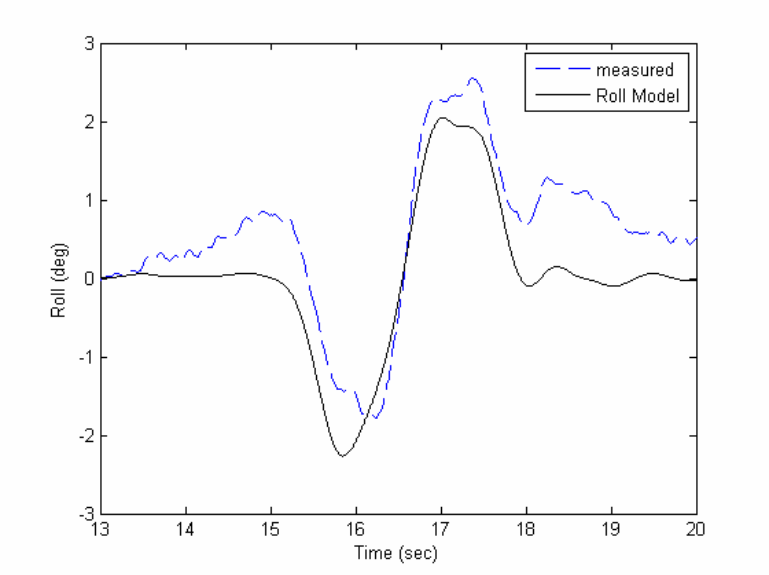

Fig. **4.17**: Roll Angle Response – Lane Change

4.3 Terrain Influence

Throughout the course of the validation process, it was noted that there were repeated irregularities in the steady-state circle data. These irregularities were similar in size, and when investigated, were determined to occur at the same geographic location. These disturbances were due to small variations of the terrain of the test track facility. Most noticeable was a small dip that was purposely created in the skid pad area to increase water drainage. This dip, however, proved to have an effect on a vehicles behavior at high speeds.

Carrying this knowledge over to transient testing, additional tests were done to consider the degree of terrain influence. For lane change maneuvers, safety cones were set up at the track to make the maneuver highly repeatable. The lane change was first completed at 5 mph and the response recorded. The lane change was then completed at the normal test speed of 25 mph and again, the response was recorded. Using the geographic position of the vehicle obtained from the GPS measurements, the vehicle

response at both low and high speed could be compared for a given spot on the track. The roll angle observed during the low speed testing was assumed to be a result of terrain disturbances, not vehicle dynamics, so any roll angle observed was then subtracted off of the roll angle measured at high speed. The two roll angles observed for the same lane change at both high and low speed is shown in Figure **4.18**

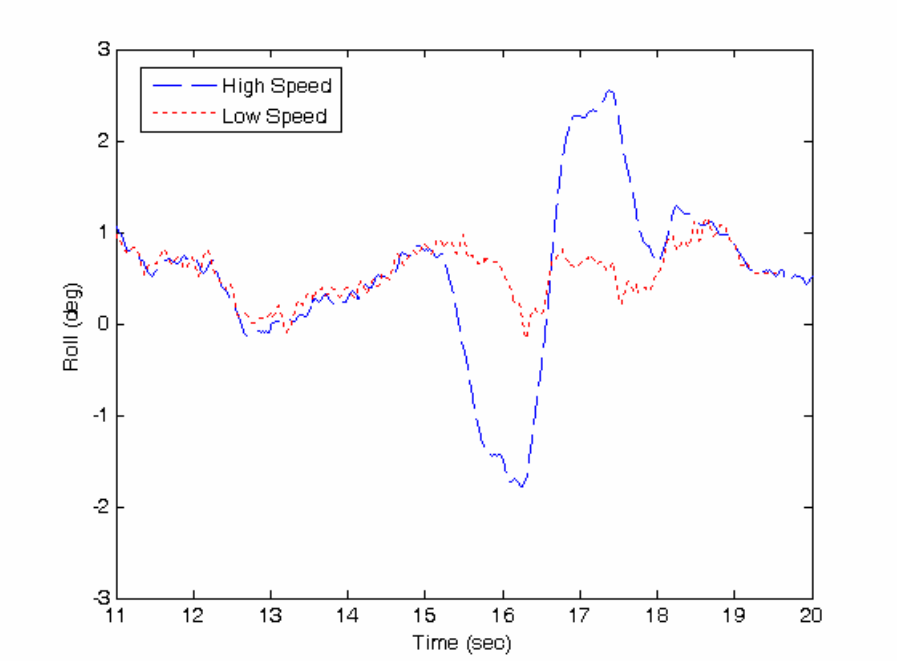

Fig. **4.18**: Roll Angle During High and Low Speed Lane Change

Figure **4.19** shows the measured roll angle during a high speed lane change along with the corrected roll angle and the roll angle predicted by the roll model. The roll angle when corrected for terrain provides a much better match to the roll angle predicted from the roll model. One can see that the terrain influences from a seemingly level surface are significant and should not be ignored.

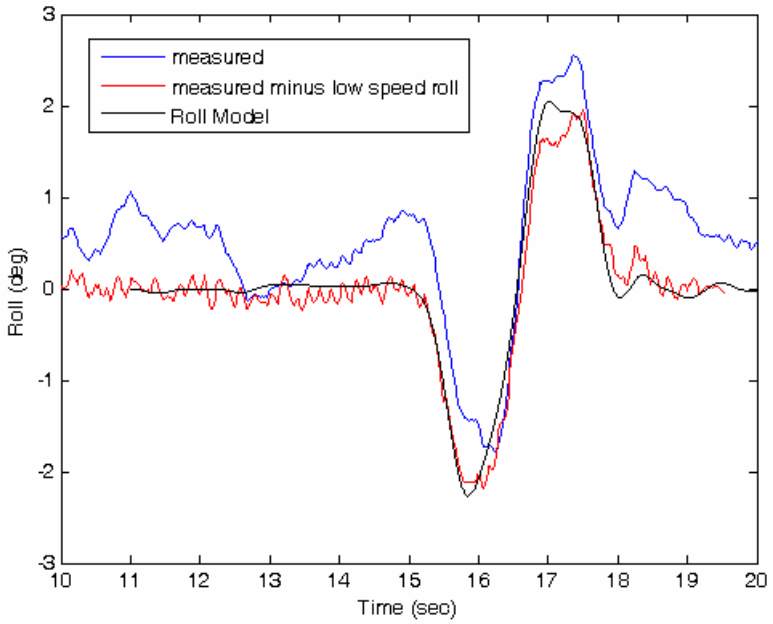

Fig. **4.19**: Corrected Roll Angle vs. Model Prediction

To better illustrate the influence of changing terrain on the dynamic response of a vehicle, lane change maneuvers were performed on a banked curve and then compared to a lane change on straight, level ground. Both maneuvers were guided by the placement of safety cones on the test track facility. The spacing between cones directing vehicle travel were measured and equated for both maneuvers. The maneuvers on the banked turn were performed such that the vehicle started in the inside lane and moved to the outside, or up the bank, during the lane change. To navigate the turn even when not changing lanes, the vehicle will require a constant steering input. The vehicle also maintains a constant roll angle throughout the turn due to the terrain. This would be in addition to any roll angle produced by an additional steering input. These offsets, a constant steering input and a constant roll angle, were determined during a baseline test that involved completing the curve without any lane change at the normal test speed of 25 mph. The roll angle and steering input measured during this baseline test were averaged and then used as offsets due to the bank of the roadway and the curvature of the road. The baseline test was performed in the middle of the roadway in an attempt to capture the average values of roadway curvature and bank angle. The average roll angle was measured to be -5.0365°

while the average steering angle measured at the tire was -1.35°. Figure **4.20** shows the raw roll angle measured during the lane change on the banked turn, and the corrected value.

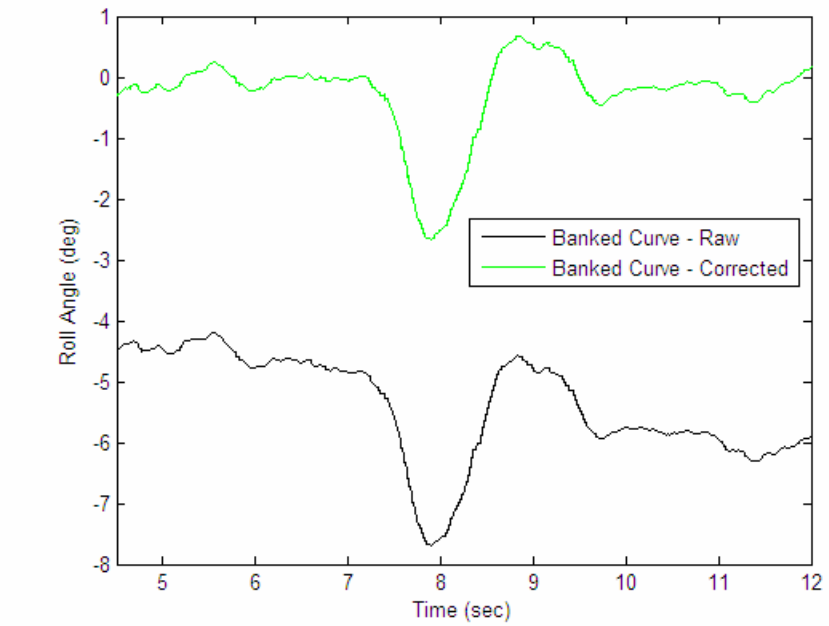

Fig. **4.20**: Measured and Corrected Roll Angle on a Banked Turn

By subtracting these offsets from the measured data, the intent is to relate measurements on a banked surface to the vehicle response during a straight and level lane change. As a result, any discrepancies between the measured response and the model prediction could more easily be detected.

Figure **4.21** shows the measured roll angle minus the terrain offset versus the roll model prediction for flat terrain from the corrected steering input measured during the banked lane change.

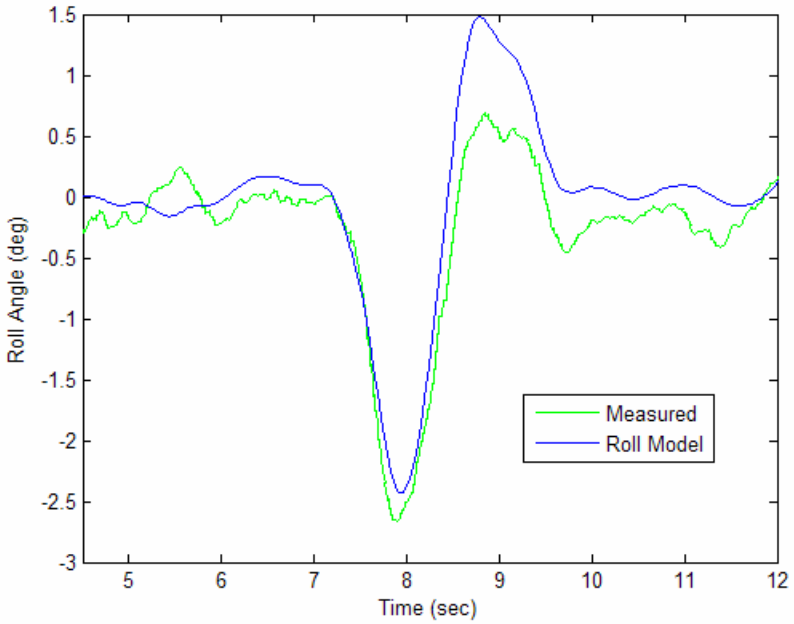

Fig. **4.21**: Measured vs. Predicted Roll Angle on a Banked Turn

The corrected steering input results in an accurate prediction of roll angle during the initial turn into the outer lane and up the incline, but overestimates the roll angle during the second turn performed in the outer lane to straighten the vehicle. In an effort to understand the reason for the discrepancy, the steering angle required to navigate the lane change maneuver on the banked turn was plotted against the steering input required to make a lane change on straight, level ground. Figure **4.22** shows the comparison between the two steering inputs.

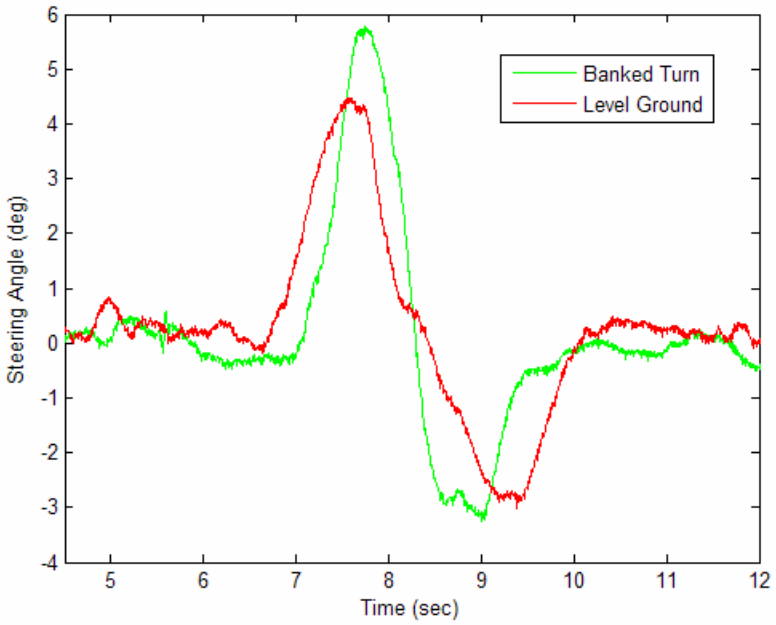

Fig. **4.22**: Measured Steering Angle Input During Level and Banked Lane Change

More steering input is required to navigate the initial turn in a lane change on a banked turn as compared to one on straight, level terrain. This could be due to the slope of the terrain, or the curvature of the roadway. The steering angle required to straighten the vehicle once in the new lane is comparable in both situations.

Noting the similarities and differences between the steering inputs required to navigate either a straight and level or banked and curved lane change maneuver can shed light on the differences observed in the vehicle response measured during both maneuvers. Figure **4.23** shows the measured roll angle minus the terrain offset on the banked curve and the roll angle measured during the level lane change.

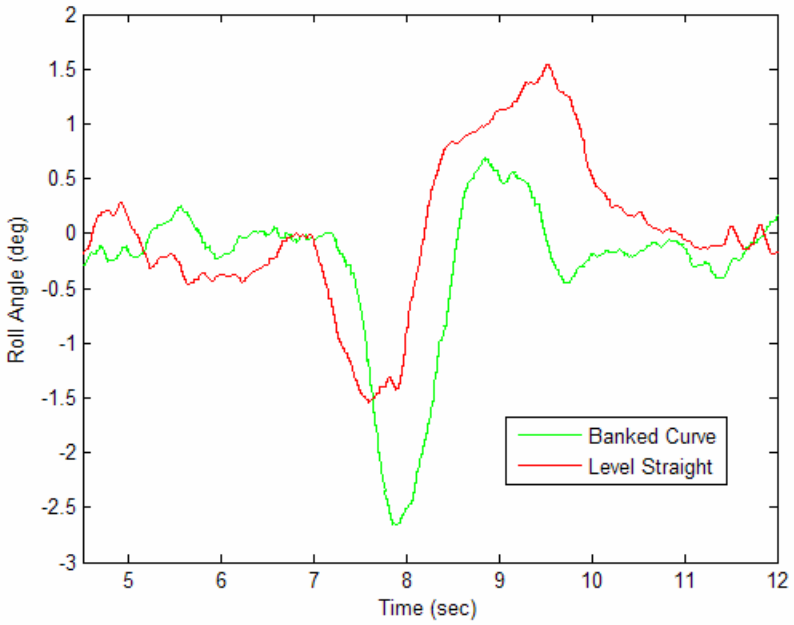

Fig. **4.23**: Measured Roll Angle During Level and Banked Lane Change

The discrepancy in roll angle during the initial turn is expected since the steering inputs required during the initial turn were different, but the roll angle during the second turn on the banked curve is lower than on level ground even though the steering input for both situations were comparable. This difference is due to the terrain resisting the rolling motion of the vehicle which would normally be induced by the supplied steering angle. This becomes evident when comparing the model prediction of roll angle with the measured roll angle of both maneuvers. Figure **4.24** summarizes the ideas presented above.

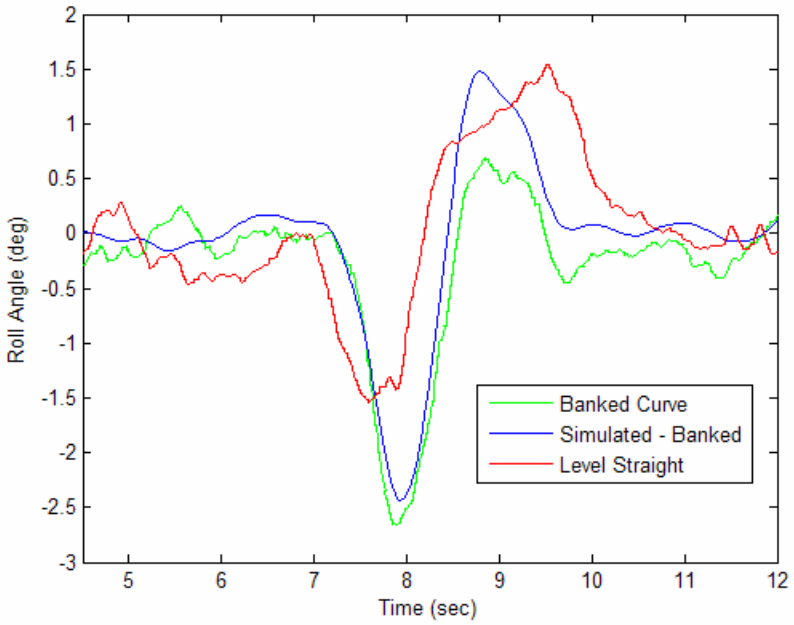

Fig. **4.24**: Measured Roll Angle During Level and Banked Lane Change vs. Predicted

A larger steering input is provided to the vehicle traversing the banked and curved lane change during the initial turn, resulting in a larger predicted roll angle which matches the measured data. Steering inputs similar in magnitude are supplied to the vehicle in both the banked and level situations during the corrective steer, but the measured roll angle on the banked turn is lower due to the terrain resisting the vehicle's motion.

4.4 Need for More Complex Dynamic Model

While the linear bicycle model does a very good job at capturing chassis dynamics of vehicles, the previous terrain and model analysis reveals that is it not suitable for all occasions, especially avoidance maneuvers that encounter changes in terrain or have high frequency steering inputs at large vehicle speeds. The addition of roll dynamics, a dynamic tire model and tire camber increased the accuracy of the model during such maneuvers but even with such corrections, the model alone cannot account

for terrain influence. To make a true comparison between model prediction and experimental data, a simulation model is needed that includes additional factors such as terrain.

1. Martini, R.D., *GPS/INS Sensing Coordination for Vehicle State Identification and Road Grade Positioning*, in *Department of Mechanical and Nuclear Engineering*. 2006, Pennsylvania State University: University Park.
2. Cameron, J.T., *Vehicle Dynamic Modeling for the Prediction and Prevention of Vehicle Rollover*, in *Mechanical Engineering*. 2005, Pennsylvania State University: University Park.
3. Karnopp, D., *Vehicle Stability*. 2004, New York: Marcel Dekker, Inc.
4. Heydinger, G.J., Garrott, W.R., Chrstos, J.P., Guenther, D.A., *Dynamic Effects of Tire Lag on Simulation Yaw Rate Predictions.* Journal of Dynamic Systems, Measurement and Control, 1994. **116**(2): p. 249-256.
5. Bundorf, R.T., *A Primer on Vehicle Directional Control*. 1968, Warren: General Motors Technical Center: Michigan Engineering Publication.
6. Gillespie, T.D., *Fundamentals of Vehicle Dynamics*. 1992, Warrendale, PA: Society of Automotive Engineers, Inc.

Chapter 5

Simulations of Vehicles During Median Encroachments

As discussed in Chapter 1, trucks, SUV's and vans are more than twice as likely to be involved in rollover accidents as passenger vehicles [1]. The National Highway Traffic Safety Administration (NHTSA) estimates that 90% of rollover accidents are tripped events, often induced by the vehicle leaving the roadway [2]. As shown in the previous chapter, terrain variations have a large effect on the dynamic response of a vehicle. To further investigate the effects of encountering changing terrain during a roadway departure, a study was performed to study the effects of median shape on the dynamic response of a vehicle. Such a study is well beyond the capabilities of the vehicle models previously presented in this work, so the commercially available simulation software, CarSim®, was utilized instead.

5.1 Methodology

A study was done to investigate parameters that affect the dynamics and location of a vehicle during median encroachments. The goal of the study was to arrive at a 'best' median profile given a variety of vehicle and driver inputs. For a given median profile, the vehicle parameters and driver inputs considered in this study included vehicle type, median encroachment angle, the vehicle's departure speed into the median, the driver's steering input and the driver's braking input. While CarSim® comes with many standard road profiles, vehicle configurations, and driver inputs; they are all intended to model normal on-road driving. Therefore, outside sources were found to provide the variables of interest.

Variations in median profiles examined in this study included changing the median width and the slopes of the front and back slope. All median profiles used were

based on the standard median profile described by the Pennsylvania Department of Transportation [3], a profile also employed by a majority of state DOTs.

Vehicle parameters were obtained by averaging the vehicles tested during New Car Assessment Program (NCAP) testing in 1998 [4], the last year that NHTSA published a database of vehicle parameters. These vehicles matched distributions used in similar studies and were selected as being representative of vehicles on the roadway today [5]. The vehicle parameters used to distinguish different vehicle types included mass, wheel base, track width, CG location and inertial parameters for all three axes. A summary of the vehicles used is shown in Table **5.1** below.

Table **5.1**: Representative Vehicle Parameters

Car	Sprung Mass(kg)	Wheel Base	Track Width	Front Axle to CG	CG Height	I_{xx}	I_{yy}	I_{zz}
Passenger Small	969	2.524	1.446	1.021	0.519	392.6	1632.2	1798.8
Passenger Large	1403	2.679	1.468	1.277	0.585	632.3	2749.7	2893.3
Pickup Small	1409.4	2.948	1.424	1.396	0.620	571.25	3142.75	3326.25
Pickup Large	1885.77	3.425	1.619	1.581	0.684	940.5	5344	5642.25
SUV Small	1718.48	2.683	1.496	1.350	0.688	803.33	3367	3522.17
SUV Large	2251.11	3.032	1.579	1.628	0.767	1157.25	5960.75	6111
Van	1847.46	2.947	1.589	1.480	0.698	992.33	4410.67	4617.83

The encroachment angles and departure speeds were selected to match data from a previous study of median encroachments [5]. The previous study analyzed median encroachment data to determine the frequency of roadway departures at different angles and speeds. The results yielded a breakdown of seven encroachment angles and seven vehicle speeds. The angles varied from 2.5° to 32.5° in 5° increments, and speed varied in increments of 16 km/hr from 8 km/hr to 88 km/hr and also included 115 km/hr.

Driver inputs were chosen to model the range of inputs a driver may chose during a median encroachment. The three steering inputs included two defined as steering to a target lateral point and one no steer condition. The target points were either the edge of the pavement on the shoulder of the original travel lanes or the middle of the median and both made use the CarSim® driver model. Braking input was varied between hard and light braking with ABS brakes used in both situations. Braking inputs in CarSim® are defined by the pressure applied to the brake system. In this study, hard braking was defined to be 15MPa while light braking was defined to be 5MPa.

The CarSim® software used for this study can easily be integrated with MATLAB® to perform multiple simulations with ease. A script was written in MATLAB® to cycle through all the permutations of vehicle and driving conditions: seven vehicles, seven encroachment angles, seven speeds, three steering inputs and two braking inputs for a total of 2058 simulated encroachments per profile. Each of the parameters were written into a separate input parsing file, which was then read by the CarSim® software as initial conditions, or inputs during the median incursion. Outputs of the simulations, including vehicle position, tire forces, angles of orientation, speed and accelerations, were then saved in an output file for each simulation for later post-processing. Details of the implementation can be found in Appendix A.

5.2 Weighting

To better represent real-world conditions and the frequency of different types of median incursions, the results of each simulation were weighted based on three variables, vehicle type, encroachment angle and initial speed. The encroachment angle and speed frequencies were taken from the Engineer's Manual for the Roadside Safety Analysis Program (RSAP), and the vehicle frequencies were found in the 2001 National Household Travel Survey, prepared for the U.S. Department of Transportation in 2005 [5, 6]. Table 5.2 summarizes the relative frequencies of encroachment angles and speed distributions as analyzed for the RSAP study and Table 5.3 presents the relative frequency of each vehicle model.

Table 5.2: Weighting Factor for Encroachment Angle and Speed Combination

	Departure Angle (deg)							
Initial Speed (km/hr)		2.5	7.5	12.5	17.5	22.5	27.5	32.5
	8	0.0002	0.0005	0.0005	0.0003	0.0002	0.0001	0.0002
	24	0.0049	0.0119	0.0118	0.0088	0.0057	0.0034	0.0042
	40	0.0151	0.0364	0.0359	0.0268	0.0174	0.0104	0.0127
	56	0.0215	0.0519	0.0513	0.0382	0.0248	0.0149	0.0181
	72	0.0205	0.0494	0.0488	0.0364	0.0236	0.0142	0.0173
	88	0.0152	0.0367	0.0362	0.0270	0.0176	0.0105	0.0128
	115	0.0200	0.0484	0.0478	0.0356	0.0231	0.0139	0.0169

Table 5.3: Weighting Factor for Vehicle Type

Vehicle	Weighting Factor
Small Passenger	0.089
Large Passenger	0.501
Small Pickup	0.090
Large Pickup	0.101
Small SUV	0.063
Large SUV	0.063
Van	0.093

The driver inputs of steering and braking were all equally weighted due to the lack of information available from accident reports about driver inputs.

In the final location plots, the ‘weight’, or likelihood, for each situation is shown by the size of the marker marking the end location, with a large marker indicating a more common occurrence. The linewidth of each marker in the plot was set equal to 500 times the frequency of the given simulation. To better understand the relationship between terrain and vehicle response, end locations were condensed into histogram plots of lateral distance from the roadway edge. To produce histograms that clearly illustrate the frequency of an event, each simulation was replicated by a whole number factor proportional to the weighting if the inputs, and then the entire plot was normalized to produce results in percentages of likelihood of a vehicle coming to rest at a certain location.

5.3 Results

While the simulations have the capability to output over 500 different variables, there are only a few primary variables of interest when considering the overall dynamics of vehicles during off-road incursions. Of particular interest was the forward and lateral velocity of the vehicle, the yaw and roll angle of the vehicle and the path traveled.

While CarSim® has been validated for on road maneuvers, the off-road validity is not as strong [7, 8]. Currently, no commercially available software on the market can accurately model rollover behavior through the point of vehicle body contact with the ground, and very few have the ability to account for soil penetration or tire furrowing. Part of this weakness is due to the lack of a comprehensive soil deformation model which would include lateral forces upon the tires that could lead to a tripped rollover. To correct for this shortfall, a post processing step was used to monitor the value of the vehicle's velocity and sideslip angle, β, the angle between the heading and the velocity vector of the vehicle. Previous studies have shown through experimental testing of induced rollovers, that a threshold of 45° sideslip and a minimum speed of 32.187 km/hr (20 mph) will lead to a soil tripped rollover [9, 10]. During the post processing, if a vehicle experienced 45° sideslip while the vehicle speed was above 32.187 km/hr, the traversal was earmarked as a rollover. Due to the unpredictable nature of rollover accidents, any trajectory data after the onset of rollover was ignored in later calculations that attempted to predict the end locations of vehicles.

Plotting end locations of each situation provides an understanding of where vehicles have traveled since leaving the roadway. Figure 5.1 shows the end locations of all simulations run on a 18.29m wide median with a 6H:1V front and back slope.

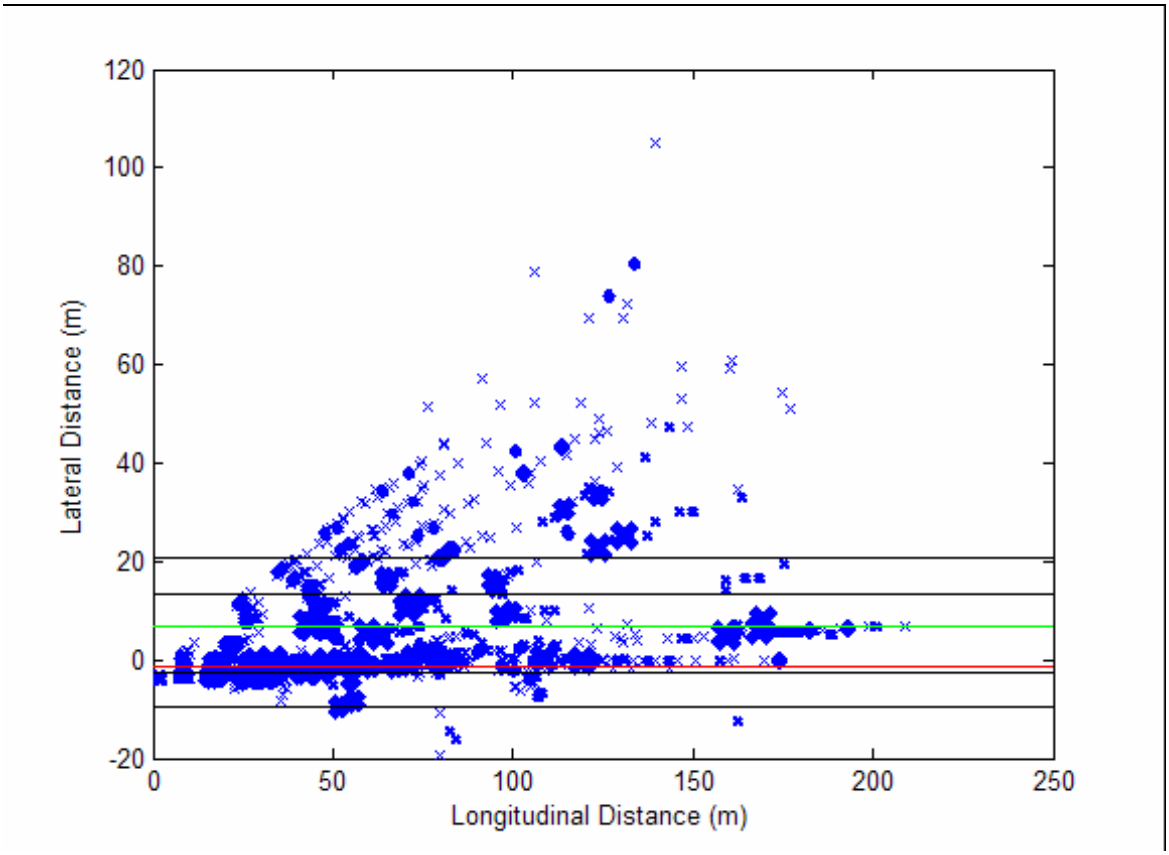

Fig. **5.1**: Final Position of all Simulations on 18.89m 6H:1V Median

The horizontal lines across the plot indicate the roadway edges and the middle of the median. The shoulder of the original travel lane ends at zero lateral offset.

As previously described, a post processing step was added to monitor vehicle sideslip angle and vehicle velocity for conditions that are conducive to vehicle rollover. The location where rollover was initiated was recorded and are plotted in Figure **5.2**, similarly to the end locations of those vehicles that did not roll.

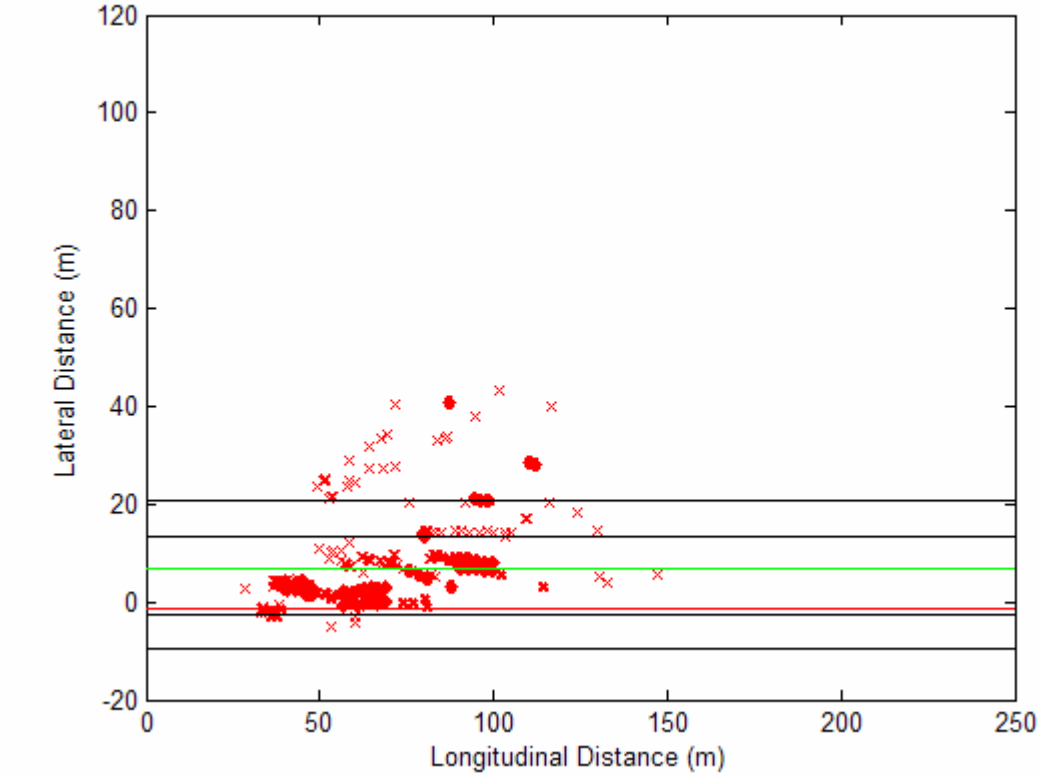

Fig. 5.2: Initiation Point of Rollover in Simulations on 18.89m 6H:1V Median

To clarify the relationship between parameters across several profiles, each profile investigated was divided into seven sections across its width regardless of the width or slope, as shown in Figure 5.3.

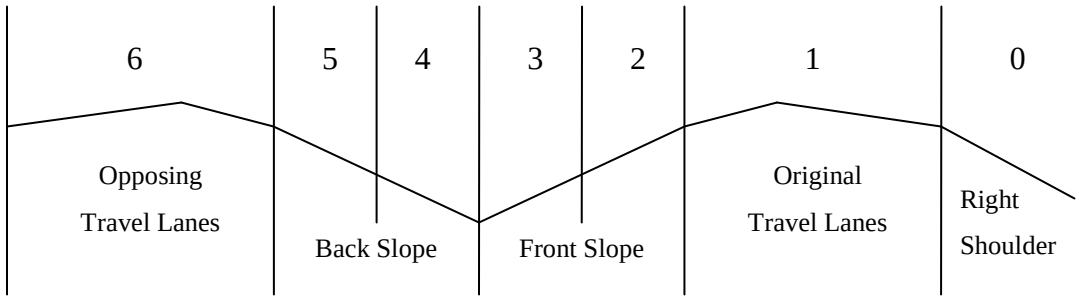

Fig. 5.3: Profile Zones

The final rest location of the vehicle or the origination of rollover were grouped into one of the above seven zones for easy comparison between different widths or slopes. If the event took place on the left side of the opposing travel lanes, it was grouped into zone six.

5.4 Sensitivity Analysis

A sensitivity analysis was performed on all five variables of interest: steering input, braking input, initial speed, encroachment angle and vehicle type. While all variables have an impact on the behavior of the vehicle during an incursion, some clearly had a more significant impact. When comparing end locations of the vehicle subject to the light and hard braking inputs, it was noted that the hard braking situations were simply a “shadow” of the light braking situations in the sense that the hard braking simulations were shifted slightly behind the corresponding simulation that received only light braking. Of all variables investigated in this study, aggressiveness of braking input seemed to have the least impact on vehicle behavior. The results from examining encroachment angle and speed were very predictable: vehicles with higher speeds traveled further longitudinally, and vehicles with larger encroachment angles and no steering input traveled the furthest laterally.

Steering input had a large impact on the severity of the dynamics of the vehicle during the median traversal. The situations in which no steering input was given to the vehicle, in general, traveled the furthest laterally. While most of the situations that received a steering input made it to the target position, either the middle of the median or the roadway edge, some resulted in a rollover or uncontrolled situation. Some situations that included a steering input did not result in the vehicle coming to a rest at the target location, but rather, the vehicle lost control and began skidding as a result of the steering input. Figure 5.4 shows the same final position plot as Figure 5.1, but distinguishes between the three different steering inputs.

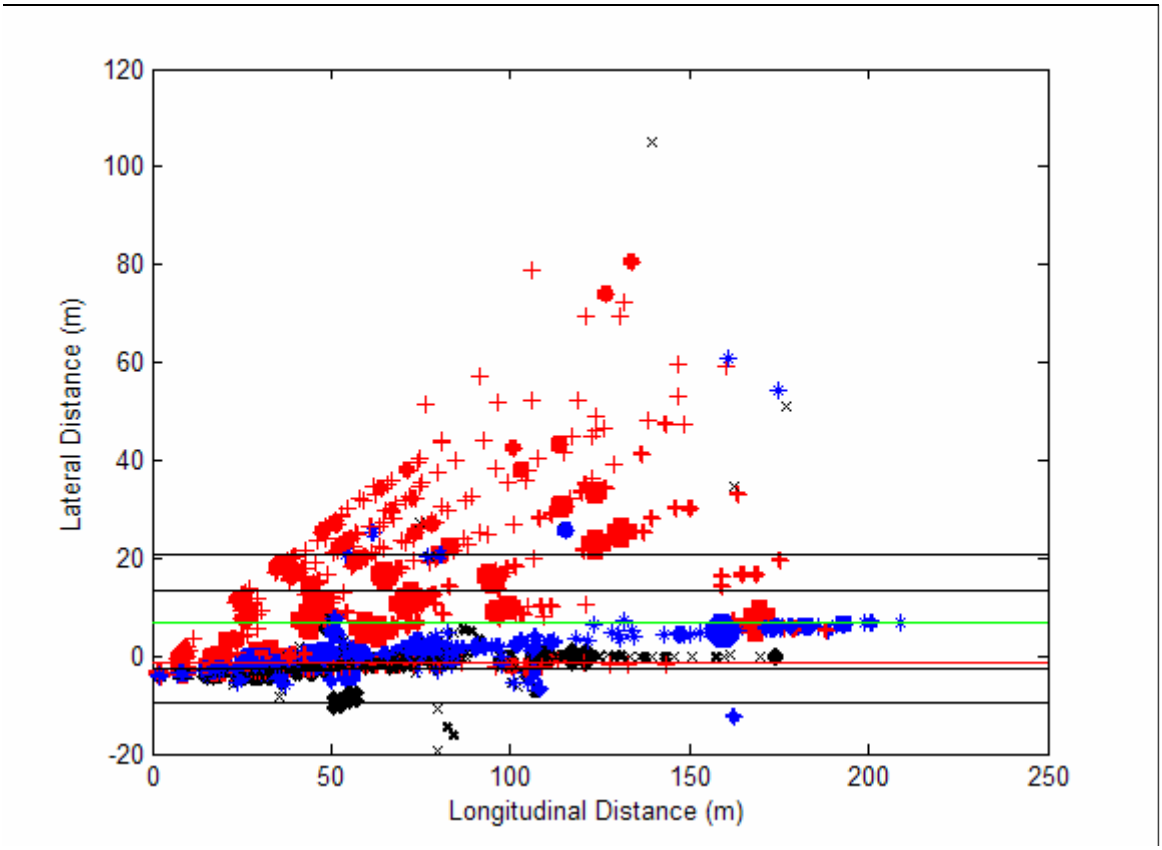

Fig. 5.4: Final Positions on 18.89m 6H:1V Median with Steering Input Distinctions

Vehicle type had a large impact on the final location of the vehicle after incursion. Larger vehicles, such as pickup trucks, SUV's and vans all traveled further laterally than passenger vehicles. Figure 5.5 shows a breakdown of end locations for each vehicle type throughout the seven zones.

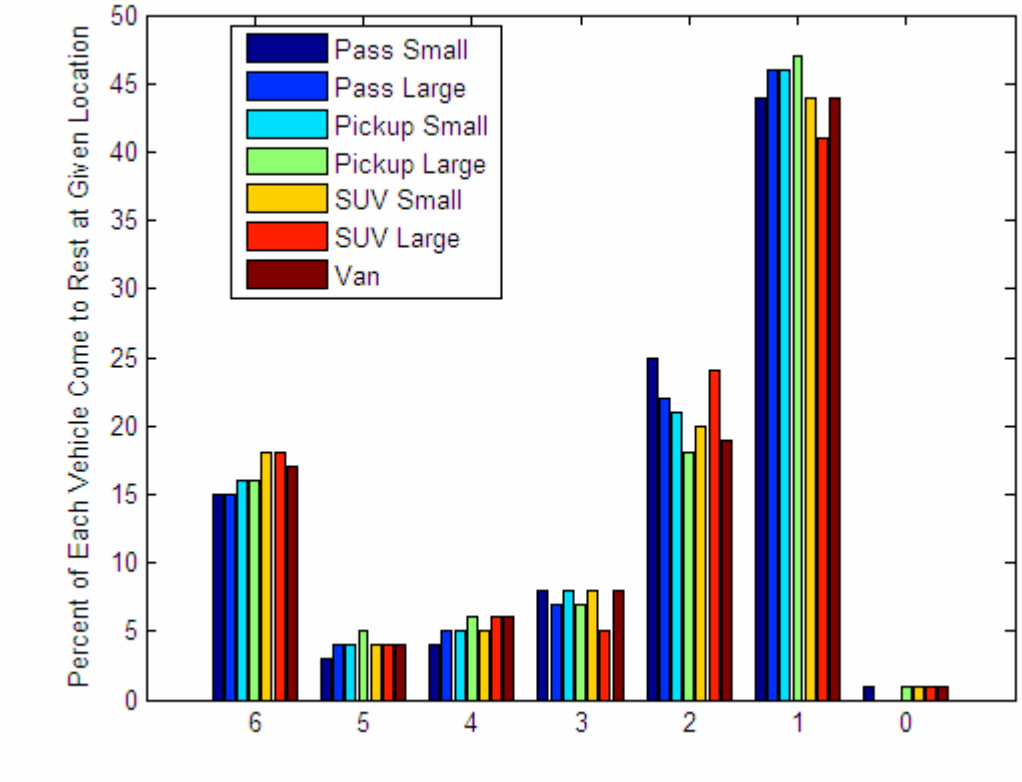

Fig. 5.5: Percent of Vehicle Type to Come to Rest Across 18.89m 6H:1V Median

The values are normalized as percentages of all incursions for a given vehicle type. As seen in the zone six distribution, there is a slight trend in the data indicating that larger vehicles are more likely to enter the opposing lanes of traffic than their smaller counterparts. As the vehicle fleet continues the shift towards larger vehicles, this distinction between vehicle size and lateral excursion into a median gains importance in redesigning the nation's roadways and off road terrain.

5.5 Profile study

Two important factors were considered during a study of median profiles, width and slope. Each was varied independently to isolate the effects of each and then the same simulations were run over all profiles. The profiles were compared by examining the end

locations of vehicles that did not rollover and the location of rollover initiation for vehicles that did rollover.

5.5.1 Varying Width

A representative median with shoulder characteristics matching the typical median from the Pennsylvania Department of Transportation and a 6H:1V front and back slope was varied in width from 12.19m (40ft) to 23.16m (76ft) in 1.83m (6ft) increments. The end locations of each simulated median incursion were recorded and weighted as described above. All medians were then compared by plotting the percentage of vehicles to come to a rest in certain lateral zones, such as the front slope, back slope and opposing lanes. Results are shown in Figure 5.6.

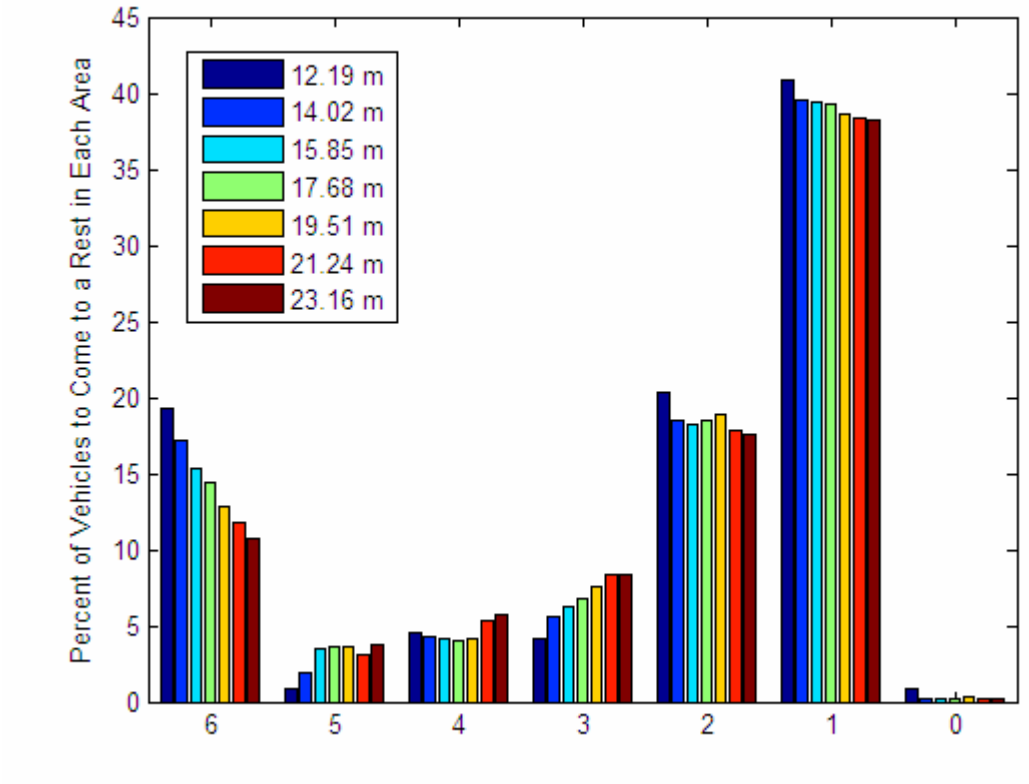

Fig. 5.6: Percent of Vehicles to Come to Rest Across Profiles of Varying Width

It is clear from the data that as the width of the median increases, fewer vehicles traverse the entire median and enter the opposing lanes of traffic. This is as expected.

But what is not expected is the influence of median width on the initiation of a rollover event. Figure 5.7 shows the percentage of rollover events in each of the seven zones for medians of varying width.

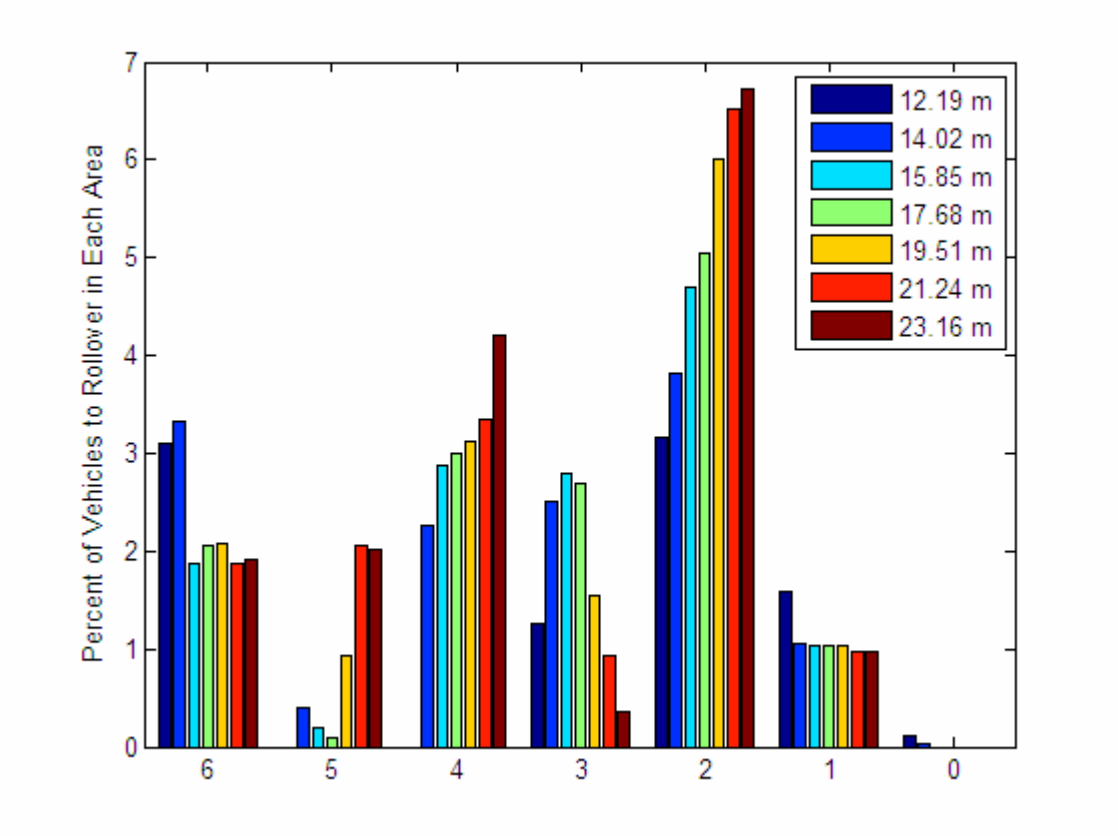

Fig. 5.7: Percent of Incursions that Lead to Rollover Across Profiles of Varying Width

The widest median, at 23.16m, results in a relatively high number of rollover situations when the vehicle leaves the roadway, and again when passing through the bottom of the v-shape. The narrowest median causes rollover in contrasting locations, the front slope and in opposing traffic. Since the goal of this study is to arrive at the 'best' median design, one that limits rollover accidents and prevents cross median collisions, the overall frequency of each was compared across medians of varying width. Figure 5.8 shows the rollover frequency for the seven medians of varying width.

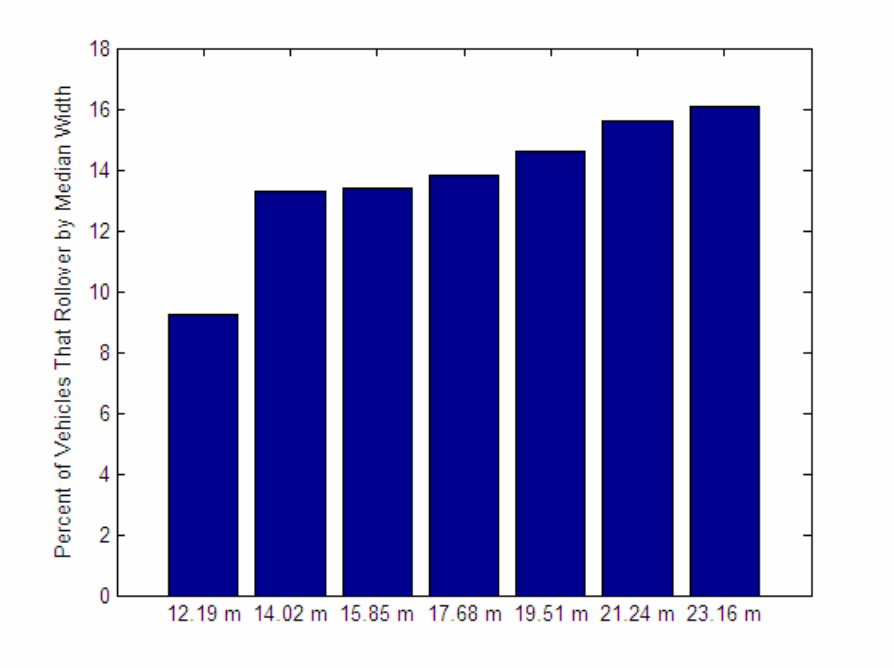

Fig. **5.8**: Percent of Encroachments that Result in Rollover for Medians of Varying Width

While it appears that a narrow median would be a good design in terms of limiting rollover accidents, Figure **5.6** showed that narrow medians result in a high percentage of vehicles crossing into opposing traffic. To balance the two worst case scenarios, of rollover and entering oncoming traffic, a ratio between rollovers occurring in the median and vehicles either entering oncoming traffic lanes or rolling over in the opposing lanes was determined. The breakdown of events formulating this ratio are shown in Eq. **5.1**

$$\text{ratio} = \frac{\#\text{ of Rollovers in Opposing Lanes} + \#\text{ Vehicles Entering Opposing Lanes}}{\#\text{ of Rollovers in Median}} \qquad \text{Eq } \mathbf{5.1}$$

For medians of varying widths, this ratio is shown in Figure **5.9**

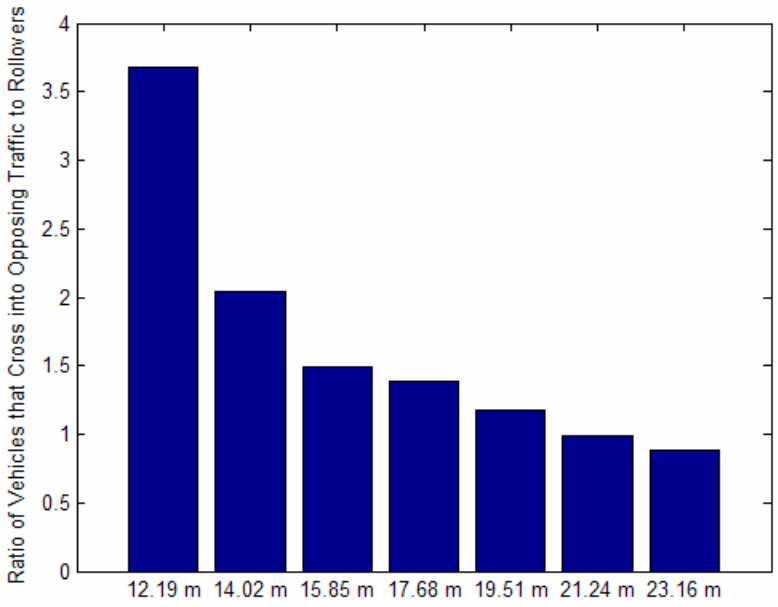

Fig. **5.9**: Ratio Between Vehicles Entering Opposing Lanes and Vehicles Rolling Over

A vehicle entering a median 12.19m in width is over 3.5 times more likely to cross into oncoming traffic than rollover, so even though the rollover frequency for a median of that width is low, the vehicle still carries a high likelihood of being involved in an accident.

As previously mentioned, a large motivating factor for comparing median profiles of different shapes is the trend of increasing vehicle size. The simulations that were identified as potentially leading to a rollover were grouped by median width in Figure **5.8**. These events were then sorted by the vehicle type involved to determine how vehicle size affects rollover propensity during a median traversal. Figure **5.10** shows the breakdown of rollover frequency by vehicle.

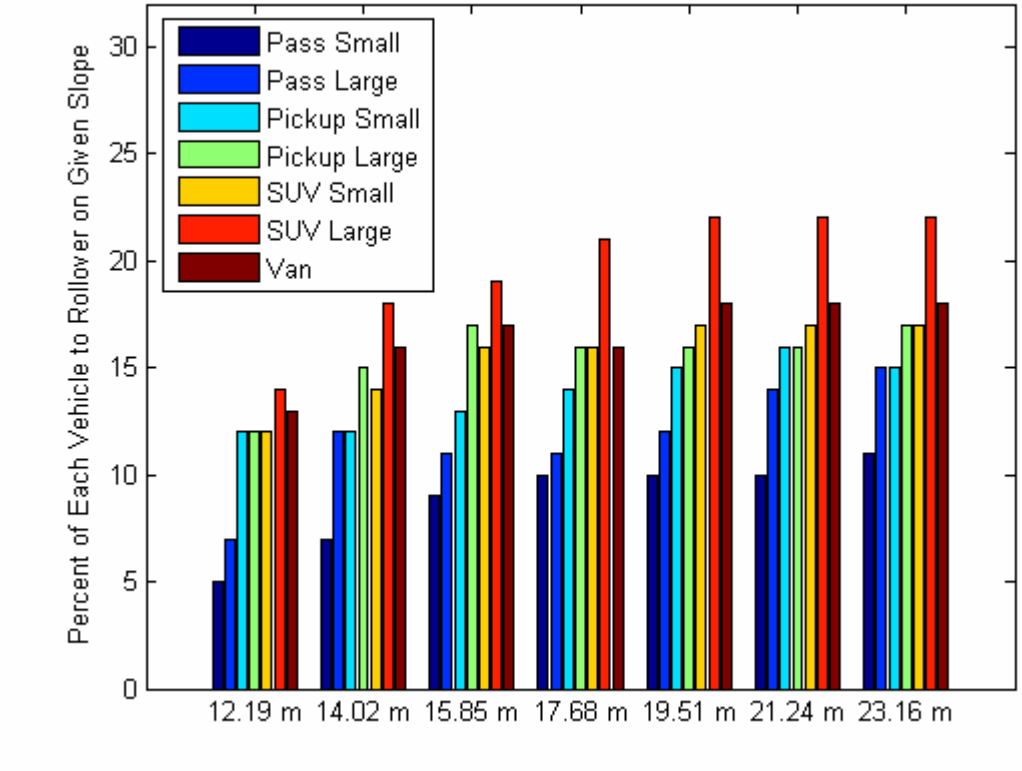

Fig. **5.10**: Rollover Frequency by Vehicle for Medians of Varying Width

It is clear that the larger vehicles have a much higher likelihood of rolling over compared to passenger cars. This trend is evident across medians of any width.

5.5.2 Varying Slope

Similarly to the varying width investigation, a representative median with shoulder characteristics matching the typical Pennsylvania Department of Transportation 18.89m wide median was altered to vary the front and back slope from a 4H:1V to a 10H:1V slope in 1H increments. The end locations of each simulated median incursion were recorded and weighted as described above. All medians were then compared by plotting the percentage of vehicles to come to a rest in certain lateral zones, such as the

front slope, back slope and opposing lanes. All seven median profiles were plotted on the same graph, Figure **5.11**.

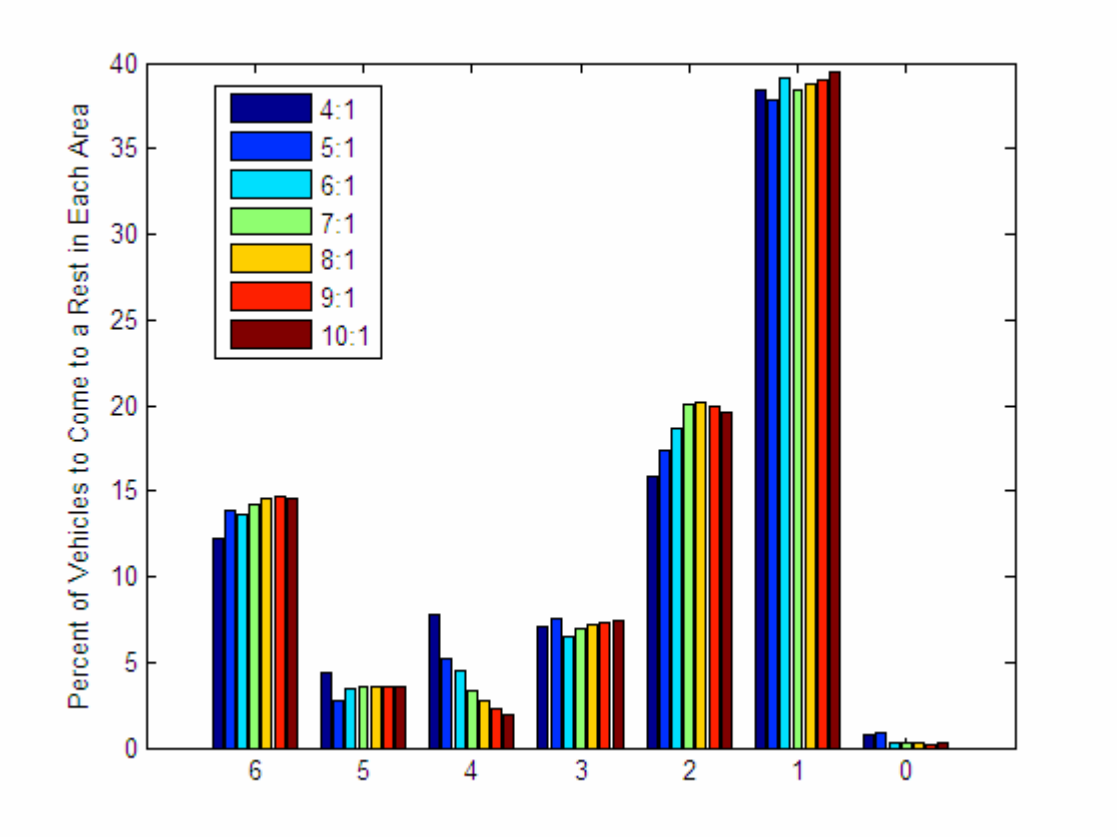

Fig. **5.11**: Percent of Vehicles to Come to Rest Across Profile of Varying Slope

The end locations do not show an obvious trend to indicate that one slope profile is more preferred over another, but a closer look at the situations that would likely lead to a rollover situation provide better proof that a safety improvement occurs for a slope no steeper than 7H:1V, as seen in Figure **5.12**.

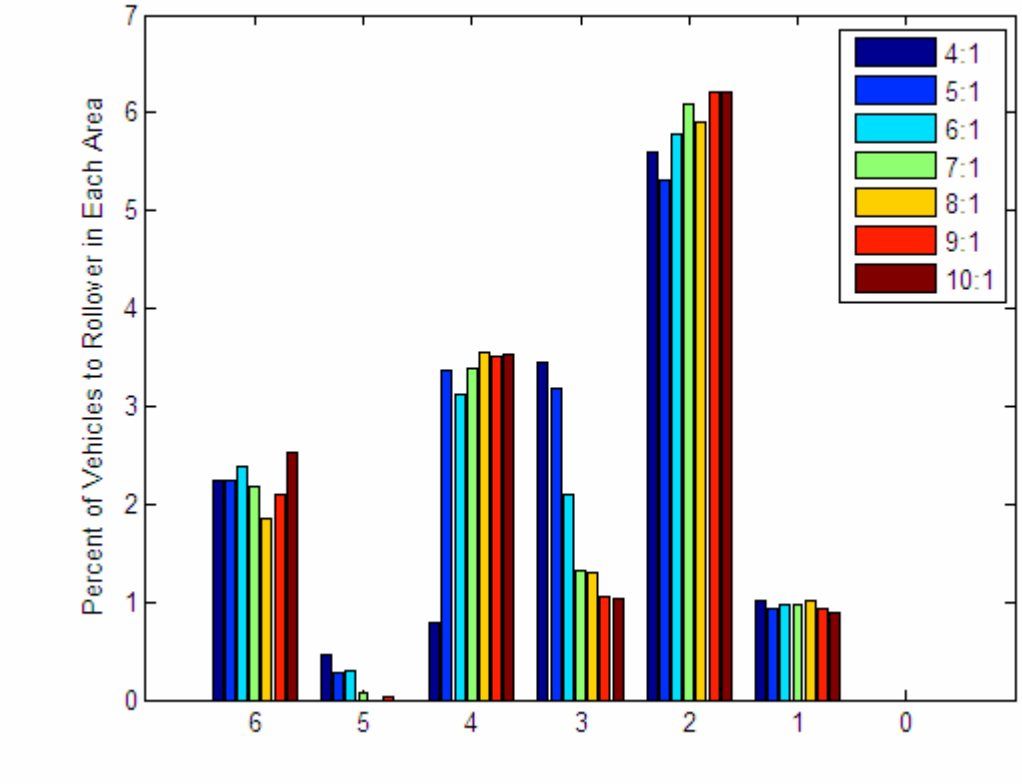

Fig. **5.12**: Percent of Incursions that Lead to Rollover Across Profiles of Varying Slope

The likelihood of a vehicle rolling over in a 18.89m width median seems to be unaffected by the front and back slope in some areas. A shallow slope seems to cause more rollovers in the initial front slope and in opposing traffic. But this slightly higher percentage is overshadowed by the significantly higher rollover likelihood on slopes steeper than 6H:1V at the bottom of the V-shape and the peak of the back slope near the opposing lanes.

Similarly to the study on median width, the rollover frequency was lumped together across the entire median profile to better quantify the effects of median slope. Figure **5.13** shows the rollover frequency for the seven medians of varying slope.

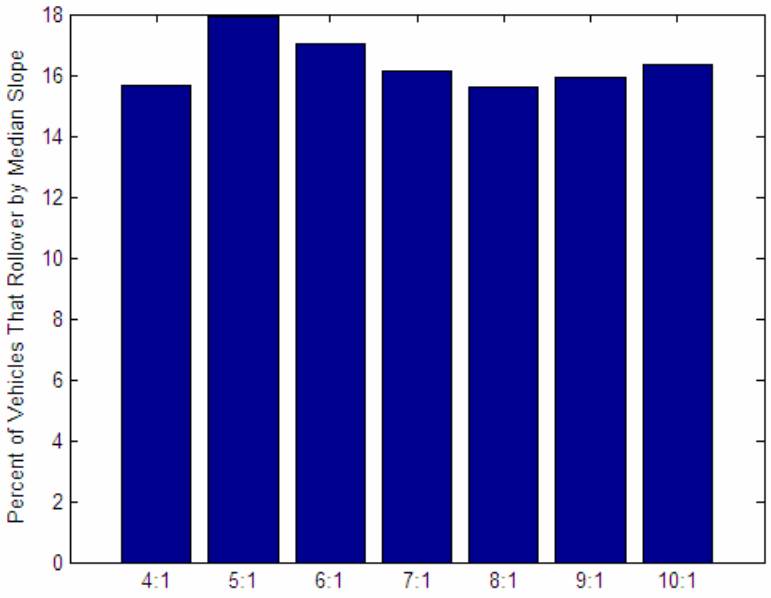

Fig. **5.13**:Percent of Encroachments that Result in Rollover for Medians of Varying Slope

An 8H:1V slope has the lowest rollover frequency, followed closely by a steep 4H:1V slope. Again, to balance the two worst case situations, the ratio between the likelihood of a vehicle entering oncoming traffic and the likelihood of vehicle rolling over in the median was calculated for each slope as in Eq. **5.1**. The resulting ratios are shown in Figure **5.14**.

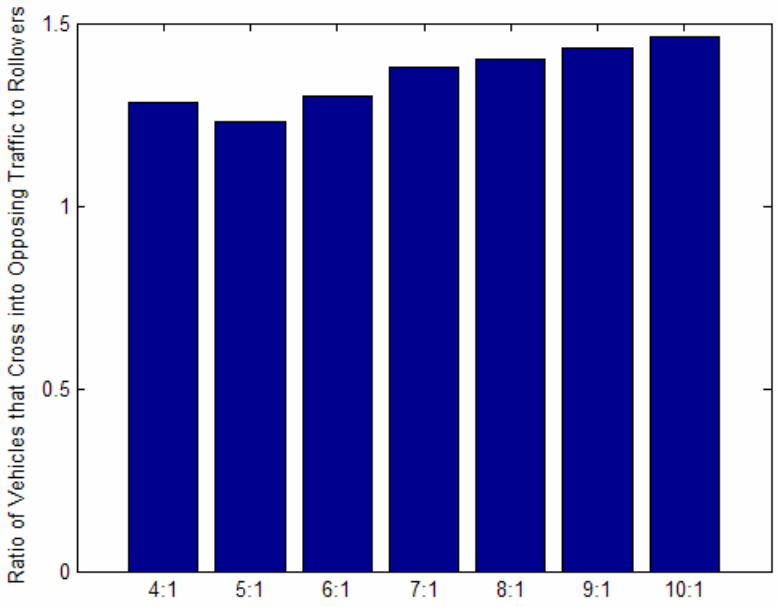

Fig. **5.14**: Ratio Between Vehicles Entering Opposing Lanes and Vehicles Rolling Over

While the 5H:1V slope has the lowest opposing lane entry versus rolling over ratio, it also has the highest rollover likelihood, although there is not a large difference between all the simulated slopes.

Again, rollover frequency was examined for the different vehicle types used in the simulation study. Figure **5.15** shows results similar to those in Figure **5.10**. Larger vehicles are more likely to rollover regardless of the slope of the median encountered.

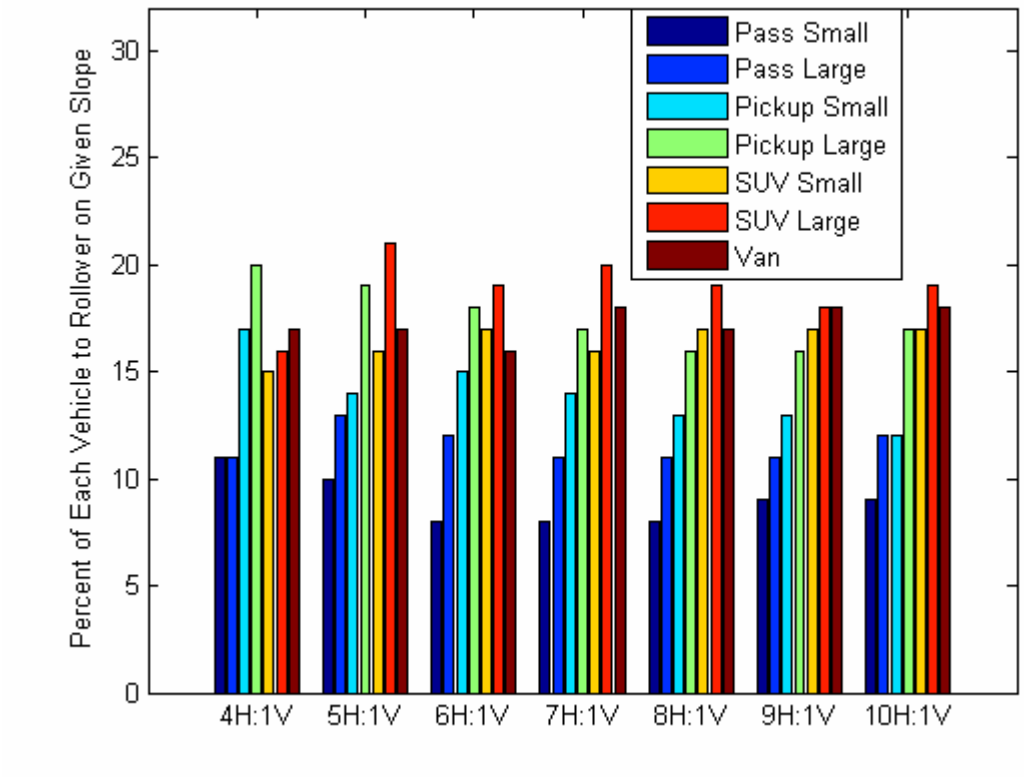

Fig. **5.15**: Rollover Frequency by Vehicle for Medians of Varying Slope

5.5.3 Summary of Findings

Through examinations of the two most significant aspects of a highway median, width and front and back slope, conclusions can be drawn through the use of vehicle dynamic simulations about safe designs and safety tradeoffs. From the comparison of the frequency of rollover accidents to the frequency of a vehicle entering into opposing lanes of travel, optimal dimensions for median design appear to be 17m (55ft) in width with 8H:1V front and back slopes. A further discussion of the results of the simulation study is presented in the following chapter.

1. *Traffic Safety Facts 2005: A Compilation of Motor Vehicles Crash Data from the Fatality Analysis Reporting System and the General Estimates System*. 2006, U.S. Department of Transportation: National Highway Traffic Safety Administration: Washington, D.C.
2. NHTSA, *Vehicle Dynamic Rollover Propensity Project Overview: http://www-nrd.nhtsa.dot.gov/vrtc/ca/rollover.htm*. 2004.
3. *Design Manual, Part 2, Highway Design*, in *13M*. 2002, Pennsylvania Department of Transportation, p. 1-24.
4. Heydinger, G.J., Bixel, Ronald A., Garrott, W. Riley, Pyne, Michael, Howe, J. Gavin, Guenther, Dennis A. *Measured Vehicle Inertial Parameters - NHTSA's Data Throught November 1998: SAE 1999-01-1336*. 1999.
5. Mak, K.K., Sicking, Dean L., *NCHRP 492 - Roadside Safety Analysis Program (RSAP) - Engineer's Manual*. 2003, Transportation Research Board: Washington, D.C.
6. *2001 National Household Travel Survey: Summary of Travel Trends*. 2004, U.S. Department of Transportation.
7. Sayers, M.W., Han, D., *A Generic Multibody Vehicle Model for Simulating Handling and Braking.* Vehicle System Dynamics Supplement, 1996. **25**: p. 599-613.
8. Chrstos, J.P., Heydinger, G.J., *Evaluation of VDANL and VDM RoAD for Predicting the Vehicle Dynamics of a 1994 Ford Taurus.* SAE 970566, 1997.
9. Kroninger, M., Lahmann, R., Lich, T., Schmid, M., Guttler, H., Huber, T., Williams, K. *A New Sensing Concept for Tripped Rollovers: SAE 2004-01-0340*. 2004.
10. Cooperrider, N.K., Hammoud, S.A., Colwell, J., *Characteristics of Soil-Tripped Rollovers.* SAE 980022, 1998.

Chapter 6

Conclusions

In this chapter, general conclusions about the work of this thesis are discussed, followed by specific conclusions about the low-order models presented in Chapter 3 and validation process described in Chapter 4. Conclusions regarding the simulation study presented in Chapter 5 are presented, followed by a discussion of possible avenues of further study.

6.1 Low Order Vehicle Dynamics Models

Chapter 3 presented derivations of the linear bicycle model including a linear tire force model using both Newtonian mechanics and Lagrange's principles. The simple model was then extended to include roll dynamics. Validation efforts first concentrated on matching the linear bicycle model to obtain values of the front and rear cornering stiffness. Utilizing a swept sine test to capture a range of input frequencies, discrepancies were noticed between the bicycle model and measured data at higher frequencies. The tire lag phenomenon was added to the linear tire model, which greatly improved the match at higher frequencies. Because the cornering stiffness values obtained during the swept sine test yielded a poor model match to steady-state behavior, camber influences were added to the tire model. An investigation of tire forces during steady-state circles indicated the tire force could be related to the roll angle of the vehicle. Roll dynamics were then added to the model and the additional parameters used in the roll model were parametrically fit to obtain an improved match between model prediction and measured data. Throughout testing, the effects of slight terrain disturbances were noticed. Repeated testing confirmed the influences and a post processing analysis allowed these effects to be removed from the raw data, vastly improving the model fits.

6.2 Simulation Study

The work presented in Chapter 5 was a preliminary study of vehicle dynamics during median incursions with the goal to show the utility of vehicle dynamic simulations for applications beyond vehicle design, such as roadway design. The commercially available vehicle dynamic simulation software, CarSim®, was used as a tool to study the effect of highway median width and slope on vehicle stability. This study was initiated as part of an effort to arrive at a more informed view of highway design.

Based on the simulation analysis, the variation in median width appears to be a more significant factor in regard to median safety than differences in median slope. There is a tradeoff in the size of medians and the type of accidents observed: narrow medians produce a high likelihood of a cross median collision occurring, yet produce fewer rollover accidents. If the goal is to balance the two harmful events, a median closer to 17m (55 ft) is suggested.

In regard to slope variations, there is not a large difference in outcomes when varying median slope. However, an 8H:1V front and back slope leads to an incrementally fewer number of rollover accidents. This suggested change away from the commonly implemented 6H:1V slope might be a reflection on the increased number of light trucks on the roadways. This study, based on modern data, indicates that light trucks such as SUV's, pickup trucks and minivans carry the highest rollover probability, regardless of median width or slope for all medians studied.

To determine the 'best' median design, other factors are needed to supplement the above conclusions. Traffic volume will affect the likelihood that a vehicle crossing into opposing lanes of traffic will be involved in an accident. Ironically, because vehicles are designed to withstand head-on and side impacts, a cross median collision may be favorable to a severe rollover accident, but the outcomes of both accident types as well as the relative impact of each type of accident are needed to truly quantify whether a median design is the 'best' in regard to vehicle safety. This work is ongoing and will continue past the completion of this thesis.

6.3 Future Work

6.3.1 Low-Order Vehicle Models

All of the experimental testing done in this thesis and in previous work was performed on the same 1992 5-door Mercury Tracer [1, 2]. To increase the confidence of the testing and validation methods presented, they should be repeated on multiple vehicles, perhaps even of different body types.

While the roll model presented in this thesis closely models the measured behavior of the vehicle, some disagreement remains. Additional sources of dynamic influence, such as suspension forces or weight transfer should be investigated to determine if inclusion of these factors will improve the model fit. But caution should be taken during such investigation to keep the models linear and add only needed complexity. The specific purpose of deriving a low-order, linear model is to utilize it for control purposes and for facilitating core understandings of vehicle dynamics. Adding complexity to the models will make the needed control theory more complicated and more expensive to implement and may obscure the respective importance of primary factors of vehicle behavior.

6.3.2 Simulation Study

Efforts were made during the simulation study of median encroachments to produce results that model behavior similar to real world conditions on the highway. Such efforts led to different steering and braking inputs and the weighting of outputs based on measured frequency of occurrence. But there are many additional factors that can influence a vehicles trajectory through a median after a roadway departure that were not included in the previous study.

The only initial conditions supplied to the vehicle prior to departure were initial speed and heading direction. This resulted in the vehicle leaving the roadway with a side

slip angle of zero, e.g. it was not skidding laterally. In reality, the driver may try to correct their motion prior to leaving the roadway, or the vehicle may be leaving the roadway as a result of an accident. Both situations are likely to cause the vehicle to be skidding or rolling to a significant degree prior to roadway departure. More simulations should be run with additional initial conditions such as vehicle sideslip to better represent possible outcomes of roadway departure.

CarSim®, the software utilized in the simulation study, cannot currently model tire furrowing or rollover behavior. While post processing steps checked for conditions that have been shown to lead to a soil-tripped rollover, actual modeling of such behavior would unquestionably lead to a better understanding of off-road vehicle behavior, especially factors that influence vehicular rollover. It is therefore suggested that the study be repeated with software that accurately models tire furrowing and rollover when such software becomes available.

The results of the simulation study could be beneficial not only to highway designers interested in median profiles, but also those interested in median barriers. The results of the study help illustrate where the installation of a barrier may be beneficial in preventing cross median collisions or vehicular rollover. By monitoring a vehicle's dynamics throughout the median incursion, information about the state of the vehicle when impacting a proposed barrier can be determined. This could be easily implemented as a post processing step to the current analysis and could lead to improved barrier testing procedures.

As previously mentioned, to obtain a true picture of the 'best' median profile, the simulation results need to be studied in a cost versus benefit analysis that includes weighting factors for accident costs as well as costs associated with installing barriers or changing the median profile. Highway designers often use such tools to determine if proposed improvements should be implemented. By examining the costs associated with the many different outcomes of a roadway departure, and the frequency of such outcomes, the 'best' solution can be determined based on financial comparisons.

Highway designers often rely on statistical data of previous implementations similar to the one proposed to determine if a change is necessary and beneficial. While

the simulations take time to set-up, run and analyze, most case studies of roadway features last at least five years to ensure accurate predictions of outcomes. But due to recent changes in vehicle fleet, the effects of vehicles increasing in size may not yet be captured in historical data. Simulation studies similar to the one presented in this work can provide highway designers with current predictions of vehicle behavior. An investigation into the rollover likelihood of a vehicle based on its size can help predict what highway designs may be more beneficial if the trend of increasing size. The use of simulation software can save money and significant amounts of time for the highway designer.

1. Martini, R.D., *GPS/INS Sensing Coordination for Vehicle State Identification and Road Grade Positioning*, in *Department of Mechanical and Nuclear Engineering*. 2006, Pennsylvania State University: University Park.
2. Cameron, J.T., *Vehicle Dynamic Modeling for the Prediction and Prevention of Vehicle Rollover*, in *Mechanical Engineering*. 2005, Pennsylvania State University: University Park.

Appendix A

Implementation of CarSim® Software

The vehicle dynamics software, CarSim®, available from Mechanical Simulation Corporation, was used in the study of median incursions presented in this thesis. An overview of the process involved in setting up and running multiple simulations with varying inputs is outlined in this Appendix.

A.1 Integration of CarSim into MATLAB

The CarSim® software is initially set up to run one simulation at a time. It has the option to save the data from one run and plot it against other previous runs, but each run would require the user to manipulate the set-up screen. To make comparisons between parameters more efficient, CarSim® has the capability to be integrated into a Simulink® model, and commanded to run through MATLAB®. Both Simulink® and MATLAB® are technical computational programs available from MathWorks, Inc. Simulink® is simulation software that is housed within MATLAB® but can also be run independently, for example, through CarSim®. MATLAB® is a computing interface and has the capability to run scripts and functions similar to C-code.

CarSim® supplies an S-function, which is a user defined block that can be placed within a Simulink® model. The CarSim® S-function contains the CarSim® solver program. This allows CarSim® to be run completely through Simulink® and can be commanded solely through the MATLAB® interface. CarSim® provides several example Simulink® models that can be used to model a variety of systems such as adaptive cruise control or active suspensions. Each of these models contains an S-function that can be copied into a new Simulink® model. The only difference between models is the CarSim® solver program used. There are 18 different solvers, all with combinations of suspension and axle configurations. The ‘Independent-Independent’

solver was used in this study. There is one input port and one output port on the S-function. If multiple inputs or outputs are specified, the signals can be combined within Simulink® by using a Mux.

The steps required to integrate CarSim® into a Simulink® model are outlined below.

1. Start in the CarSim® main Run Screen in *Bridget's Restart*
2. Set the *Model type* tab to 'Models: Transfer to Local Windows Directory.'
3. From the pull down menu, select 'File Transfer to Local Bridget.'
4. Click on the blue box which now reads 'File Transfer to Local Bridget.'
5. The vehicle solver codes are now shown on the right side of the screen. Changes can be made to the codes used.
6. The file location is shown next to the vehicle solver code. The Simulink® model to be used needs to be saved in the specified directory.
7. The *Import* and *Output* tabs both have pull down menus next to them. In each, select I/O Channels and click on the blue tab when it comes up.
8. There are several import and output files that come with CarSim® to be used when runing the provided Simulink® models. The *Median Export* output file was used in this study. Details of the import and output channels available can be found clicking on the file name and then by clicking 'View File' at the top of the new screen. The order of the inputs and outputs should match the vertical order of the input or output signals going to or coming from the S-function in the Simulink® model.
9. There is a large box on the left side of the screen where external files can be specified. This is where the input parameter files used in this study are specified, for example 'INCLUDE Sim_ICs.par.'
10. For this simulation study, seven files were needed. They were:
    a. Sim_ICs.par
    b. Brake.par
    c. Steer.par
    d. Speed.par

e. Encroach.par
f. Vehicle.par
g. Median.par

11. Click the back arrow to return to the main run screen.
12. Click the *Send* button, wait approximately 5 seconds and then click the *Receive* button. This establishes connections between the specified files. It also transfers the time step specified in the middle of the CarSim® screen to the Simulink® model.

At the time of this writing, the S-functions are only set up to run in an old version of MATLAB®. They also only work if MATLAB® is opened through CarSim®. To do this, select 'Models: Simulink' in the *Models Type* tab. Choose any model from the list and a box with *Open Model* should appear. Clicking that box will open the chosen Simulink® model, but also the correct version of MATLAB®. The Simulink® model is no longer needed, but any scripts will need to be opened in this version of MATLAB®. Make sure to re-select Models: Transfer to Local Windows Directory' and click the *Send* and *Receive* buttons again before starting the simulations.

A.2 Specification of Simulation Variables

A MATLAB® m-file, *script_runCarSim.m*, was created to run through the desired simulations. In this script, additional m-files are called that contain information about median profiles, vehicle parameters, braking and steering inputs. These values were housed in different m-files to make the main script more manageable in size. The script is set up to cycle through seven median profiles, seven vehicle types, seven encroachment angles, seven initial speeds, three steering inputs and two braking inputs. The file is set up with multiple 'for' loops so that all iterations of one variable will be run before any other variables are changed. In the very first simulation, all variables will be set to the first specified value. Then the braking input will be changed to the second configuration, and the simulation run again. The third simulation will still have the first configuration of

profile, vehicle, encroachment angle and speed, but will have switched to the second steering input.

The variables are fed into the simulation by writing them into files which are then read by the solver. These were mentioned in step 8 above. Each variable, along with the initial vehicle conditions are written into separate parsfiles. The parsfiles are written for the initial run, but because of the 'for' loops, are rewritten only when the variable specified in the file changes. This shortens the processing time necessary for each simulation.

When writing parsfiles, the first line must always read *PARSFILE* followed by a blank line and the last line must read *END*. Some variables are entered as values correlating to specific keywords while others are entered in tabular form. Descriptions of each keyword and table can be found either in the 'Math model import list' or the 'Echo file with initial conditions.' Both can be found by selecting them from the bottom right pull down menu on the main control screen. Each table has a heading to specify what information the table contains. The heading includes the variable and the number of columns in the table.

The first parsfile written within the script does not include a varying variable, but initializes the vehicle on the roadway. In the *Sim_ICs.par* file, the *OPT_INIT_ROAD* 0 command initializes the vehicle on the roadway, accounting for any terrain variation. The initial lateral position is then set at -4.2m, which is the middle of the left traffic lane.

Next, the median profile and friction values are written in tabular form into the file *Median.par*. In the 3D median profiles and friction profiles, the first row of the table begins with a 0 as a placeholder, followed by lateral distances. The rest of the first column contains longitudinal information, and the remaining values contain either vertical or friction values. The elevation of the roadway needs to be entered into a table called *ROAD_DZ_CARPET* and the friction values are entered into a table called *MU_ROAD_CARPET*. Once the table values are written, the file needs to read *ENDTABLE*.

The vehicle parameters are written into the file *Vehicle.par*. All the parameters are entered as keyword specifications. Table **A.1** shows the keywords and definitions of the parameters used to specify vehicle type.

Table **A.1**: CarSim® Vehicle Parameter Keywords

CarSim® Keyword	**Vehicle Parameter**
L_WHEELBASE	Vehicle Wheelbase
L_TRACK	Vehicle Track Width
M_SU	Sprung Mass
LX_CG_SU	Front Axle to CG Distance
H_CG_SU	CG Height
IXX_SU	Roll Moment of Inertia
IYY_SU	Pitch Moment of Inertia
IZZ_SU	Yaw Moment of Inertia

The next two files written specify the encroachment angle and initial speed. The encroachment angle is written in *Encroach.par* by using the keyword *SV_YAW*, and the initial vehicle speed is written in *Speed.par* by using the keyword *SPEED*.

The steering input is written in *Steer.par* in 2D tabular form specifying input that correlates either to time or longitudinal distance. The no steer option is created by turning the driver model off by setting *OPT_DRIVER_MODEL* to 0. The steering input is then specified in a table named *STEER_SW_TABLE* to be zero for the duration of the run. The commanded steering inputs require the driver model be turned on, or set to a value of 1 and are entered in a table named *LTARG_TABLE*. The input is then specified to correlate to the longitudinal distance traveled, with either the goal of returning to the shoulder of the roadway, or the middle of the median.

The last file created controls the braking input. The brake pressure versus time is input in a 2D table named *PBK_CON_TABLE* and written to the file *Brake.par*.

A.3 Running the Simulations

Once all the variables are specified and written into their respective parsfiles, the simulations are ready to run. As with any other Simulink® diagram, the command

run('Median_study') when entered in MATLAB® will run the Simulink® diagram saved as Median_study. The *script_runCarSim.m* file calls this command and then saves outputs from the simulation into a structure called *data*. A simulation ID is also saved, indicating which variables were used in each run. This will be helpful in post processing of the data.

Because the output files are rather large, the *data* structure is saved after the simulations have cycled through all combinations for a given vehicle. This includes all iterations of encroachment angle, initial speed, steering and braking input. The name of the saved file is *groupxy.mat* where x indicates the median profile and y indicates the vehicle used in the simulations in that file. The data files can be saved in any directory by specifying the path in the main m-file.

A.4 Location of Simulations Files

Currently, all the files necessary to run the simulations described in this work are housed on the 8300 Dell Dimension desktop computer in Dr. Brennan's graduate student office, 323 Leonhard building. CarSim® 6.05 is the version currently installed, and all files are saved in the C:\CarSim\Programs\Simulink_MDL folder. There are seven files needed to repeat the work in this thesis, the Median_study.mdl Simulink model, and then six m-files:

- script_runCarSim.m
- script_median_profile.m
- script_median_profile16width.m
- script_median_profile60slope.m
- script_car_params.m
- script_braking_control.m

The three m-files detailing median profiles were used to keep the inputs organized. The *script_median_profile.m* file contains profile information for five median profiles used in a preliminary study performed for NCHRP 22-21. The other two were used to study the

effects of varying median width and slope. The *script_median_profile16width.m* file contains information on seven profiles, all with a 6H:1V slope, but varying in width. The *script_median_profile60slope.m* file contains information on seven profiles, all 60 feet (18.89m) in width, but with varying slopes. All of the scripts can be easily modified to change the variables used in the simulation

.